FACIES	44	1-22	Pl. 1-6	1 Fig.	3 Tab.	Erlangen 2001

Fluvial Tufa Formation in a Hard-Water Creek (Deinschwanger Bach, Franconian Alb, Germany)

Gernot **Arp**, Nicole **Wedemeyer** and Joachim **Reitner**, Göttingen

KEYWORDS: STROMATOLITES – TUFA – CYANOBACTERIA – BIOFILMS – CALCIFICATION – RECENT

Contents

Summary

Cyanobacteria-dominated biofilms involved in tufa deposition in the hardwater creek Deinschwanger Bach, Bavaria, were investigated with regard to their effect on the carbonate equilibrium and fabric formation. Current tufa deposition is evident by up to 1.5 mm thick crusts that have formed on substrate plates placed in the creek for 10 months. Hydrochemistry data indicate that carbonate precipitation along the creek is physicochemically driven by CO_2 degassing, whereas photosynthetic carbon assimilation is without detectable effect on the macroscale carbonate equilibrium. However, stable isotope data indicate a minor photosynthetic effect, but only for the lower creek section where the pCO_2 already drops to the two-fold of the atmospheric level. Though the initial process of external nucleation on cyanobacterial sheaths in the lower creek section might be promoted of by a photosynthetically-induced microscale pH gradient, the effect is not strong enough to cause a $CaCO_3$ impregnation of the sheaths. The fabric of the laminated tufa crusts in the creek reflects the temporal alternation of porous microsparitic *Phormidium incrustatum - Phormidium foveolarum* - diatom biofilms in spring, micrite-impregnated *Phormidium incrustatum - Phormidium foveolarum* - diatom biofilms in summer-autumn, and detritus-rich non-calcified diatom-biofilms in winter. By contrast, exopolymer-poor surfaces of cascade tufa mosses show large, euhedral spar crystals. Non-phototrophic bacteria, which occur in large numbers in *Phormidium incrustatum - Phormidium foveolarum* - diatom - communities, thrive on extracellular polymeric substances (EPS) and dead cells of the cyanobacteria and are unlikely to promote $CaCO_3$ precipitation.

1 CALCAREOUS TUFA FORMATION AT COOL SPRINGS AND IN CREEKS

Calcareous tufa deposits of springs and creeks are a common feature of karst regions such as the Franconian and Swabian Alb (e.g., Stirn, 1964; Grüninger, 1965). Karstification driven by soil-derived CO_2 leads to the formation of Ca^{2+}-rich, high-pCO_2-groundwaters which rapidly degas when the aquifer discharges to the subaerial environment (see, e.g., Bögli, 1978). Calcareous tufa refers to porous, poorly stratified, usually friable carbonate rocks which form at such non-thermal springs and creeks. Low-Mg-calcite is usually the main mineral component (e.g., Irion & Müller, 1968) because of generally low Mg^{2+}/Ca^{2+} ratios of karst waters.

The formation of calcareous tufa at springs and creeks is generally considered to be largely inorganic, i.e. physicochemically driven by CO_2 degassing rising $CaCO_3$ supersaturation (e.g. Herman & Lorah, 1987, 1988). In addition, mosses and plants that populate springs and creeks provide large surfaces, thereby enhancing CO_2 degassing. Cyanobacteria are considered to provide suitable nucleation sites by their sheaths (Pentecost, 1985; Pentecost & Riding, 1986). In addition, their sticky sheaths should trap and bind detrital carbonate particles, which further grow inorganically within the supersaturated environment. The potential influence of metabolic CO_2 fixation by plants and cyanobacteria is mentioned in almost any study on tufa systems. Pia (1926, 1933) and Wallner (1934ab, 1935) denoted some tufa deposits as "physiologically precipitated" or "phytogen", caused by CO_2 assimilation. Golubic (1973) noted that $CaCO_3$ precipitation in the upper part of a river flow is largely inorganic, whereas biogenic precipitation may increase downstream when equilibrium conditions with regard to atmospheric pCO_2 are reached. Indeed, tufa depositing springs and creeks show only

Addresses: Dr. G. Arp, Dipl.-Geol. N. Wedemeyer, Prof. Dr. J. Reitner, Institut und Museum für Geologie und Paläontologie, Goldschmidtstraße 3, D-37077 Göttingen, Germany, Fax: +49-551-397918, email: garp@gwdg.de

minor diurnal changes in pH (Grüninger, 1965; Usdowski et al., 1979). Calcite precipitates of a tufa depositing creek north of Göttingen show $\delta^{13}C$ values close to that of the dissolved carbonate species, thus, indicate a rapid precipitation to cause this isotopic disequilibrium (Usdowski et al., 1979). Further, photosynthetic rates of cyanobacteria measured by ^{14}C uptake were too low to account for $CaCO_3$ deposition rates observed in tufa systems (Pentecost, 1978). Only about 1-5% of the $CaCO_3$ could have formed as a result of cyanobacterial CO_2 uptake in the case studies investigated by Pentecost (1978). Nonetheless, under conditions of low discharge photosynthesis determines the diurnal variations in $\delta^{13}C$ in dissolved inorganic carbon in creeks (Spiro & Pentecost, 1991).

All these three observations clearly point to a negligible role of photosynthetic CO_2 assimilation in shifting the carbonate equilibrium to cause $CaCO_3$ precipitation in fluvial tufa systems (e.g., Grüninger, 1965: 88). This view has recently been confirmed by a comprehensive study on water chemistry and tufa precipitation of two hardwater creeks near Bad Urach, Swabian Alb, South Germany (Merz-Preiß & Riding, 1999).

However, other studies focussed on potential microscale gradients caused by non-phototrophic bacteria, which possibly modify the carbonate equilibrium within the exopolymer matrix of cyanobacterial colonies and mats (Caudwell, 1987; Pentecost & Therry, 1988; Szulc & Smyk, 1994). Though the presence of several chemoorganotrophic and chemolithotrophic bacteria in tufa biofilms has been shown (Szulc & Smyk, 1994), data on their in-situ abundance and metabolic activity in natural samples are still missing. Aerobic heterotrophs isolated from 10 tufa-depositing sites in Europe and North-America failed to cause $CaCO_3$ precipitation in laboratory experiments (Pentecost & Therry, 1988). Most of these isolates were gram-negative, motile rods of the "*Pseudomonas*"-type. Consequently, the tufa-depositing hardwater creek Deinschwanger Bach has been investigated with regard to hydrochemistry, the effect of biofilm exopolymer matrix on $CaCO_3$ nucleation, fabric formation, and the presence of non-phototrophic bacteria.

2 ENVIRONMENTAL SETTING

The Deinschwanger Bach ("Wurstbach") is a hardwater creek located at the western rim of the Franconian Alb approximately 30 km ESE of Nürnberg (Fig. 1). The Franconian Alb plateau consists of Upper Jurassic carbonate series, which are affected by intensive karstification since the Early Cretaceous. Numerous caves, karst springs, and tufa deposits are known from this area.

The E-W trending valley of the Deinschwanger Bach cuts down from Lower Kimmeridgian limestones ("White Jurassic") down to Aalenian-Bajocian sandstones of the "Brown Jurassic" (Fig. 1). Callovian clays of 2-4 m thickness ("Ornatenton") below the up to 70 m thick Oxfordian-Kimmeridgian limestones are responsible for numerous springs discharging from the karst aquifer. A second major spring horizon is bound to clayey siltstone intercalations ("Disciteston") within the 50 m thick Aalenian-Bajocian sandstones. Large parts of the valley floor are covered by up to 6 m thick Holocene tufa deposits which now form terraces at the incised creek. The formation of Holocene tufas is possibly related to large landslides that might have dammed the creek temporarily (Schmidt-Kaler, 1974).

The main spring of the Deinschwanger Bach discharges 10 - 15 L/sec (Schmidt-Kaler, 1974). It is located at 520 m above S.L. at the eastern end of the valley, approximately 10 m above the Callovian-Oxfordian boundary. The creek is up to 3 m wide and usually less than 50 cm deep. Current $CaCO_3$ deposition starts approximately 1.2 km away from the main spring and ends approximately 2.6 km downstream. In addition, both wooded sides of the valley show several small cascade tufas and wide-spread, swampy areas covered by sheet-like deposits of carbonate encrusted shells of the pulmonate snail *Cepaea hortensis*.

Four sites have been selected for a detailed study of biofilm calcification and water chemistry (Fig. 1):

(1) The main spring (520 m above S.L.; site 1; Pl. 1/1),
(2) a small tufa cascade at the southern valley side (495 m above S.L.; site 2; Pl. 2/1),
(3) a small barrage of the middle creek, which is incised in Holocene tufa terraces (477 m above S.L.; site 3; Pl. 3/1), and
(4) a low-turbulent, well-illuminated section of the lower creek part (462 m above S.L.; site 4; Pl. 4/1).

All sampling sites, except for the lower creek section, are situated within shady, wooded area.

3 INVESTIGATED MATERIAL AND METHODS

Biofilm and water samples have been taken in spring (01.05.1996; 12.06.1999), summer (22.07.1996), autumn (22.11.1996), and winter (01.03.1997) at the four sites (Table 1). 125 hardpart sections of 21 formol/glutaraldehyde-fixed, LR-White embedded tufa biofilm samples have been investigated by conventional light microscopy and wide-field deconvolution epifluorescence microscopy. In addition, 30 sections of 11 artificial substrate plates, which have been placed at the four sites for 10 months (22.11.96 - 30.09.97), have been investigated. The 5x5 cm sized plates of Solnhofen limestone, polystyrene, wood, and iron steel were fixed by 15 cm long screws at water-covered places. Fixation and preparation of hardpart sections was done as described in Arp et al. (1998). For details of Wide-field deconvolution epifluorescence microscopy (WDEM) see Manz et al. (2000). 11 semithin and 9 ultrathin sections of two decalcified samples were prepared for TEM studies (sample preparation see Arp et al., 1999). The ultrathin sections were examined at a Jeol 100 B transmission electron microscope at 80 kV at the Max-Planck-Institute for Biophysical Chemistry, Göttingen.

Electrical conductivity (EC), temperature, pH, and redox potential of water samples were measured in the field. For each samplings site a diurnal cycle (9.00 a.m. to 18.00 p.m.) of water temperature, oxygen, redox potential, conductivity and pH were recorded for each season in 1997. Temperature

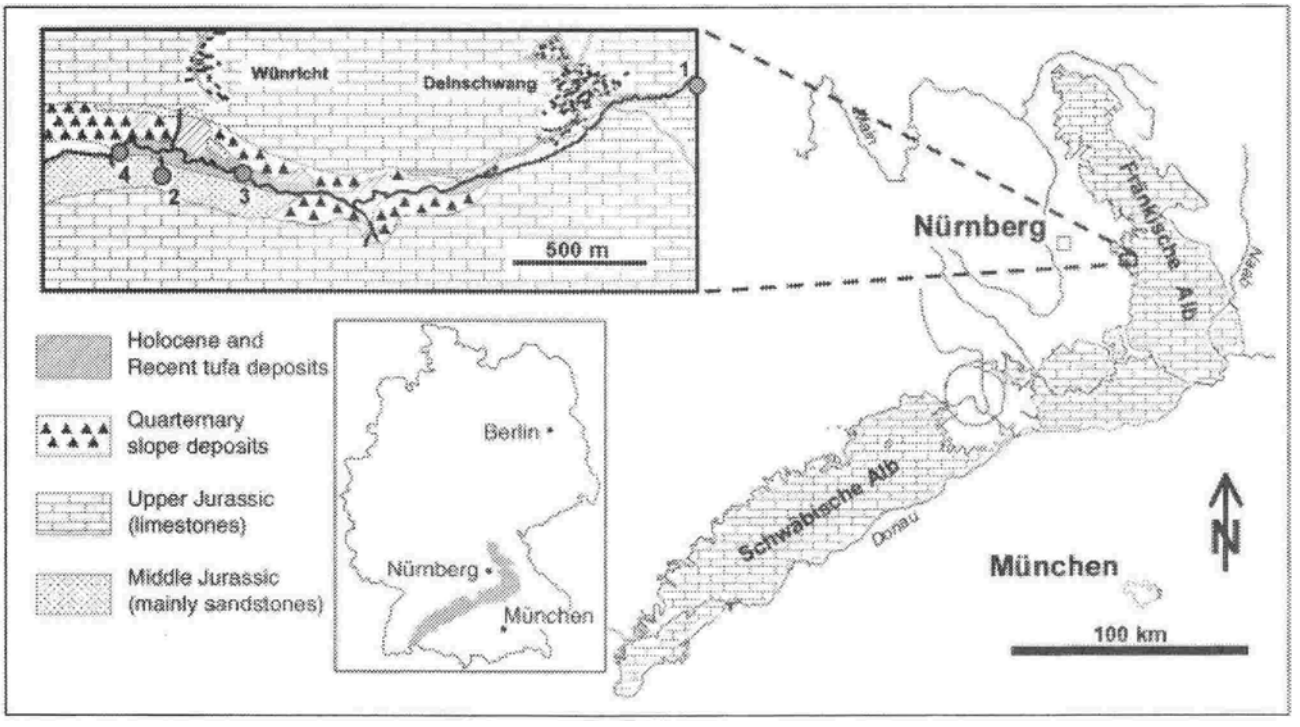

Fig. 1. Geographic situation of the hardwater creek Deinschwanger Bach at the western margin of the Franconian Alb, Bavaria. Insert shows the location of the sampling sites along the creek. Site 1 denotes the main spring, site 2 is a small tufa cascade at the southern side of the valley, site 3 and 4 denote the middle and lower creek parts.

compensated conductivity (20 °C) was determined with a LF 323 instrument (WTW Co.). Redox potential and pH were measured with a HI 9025 pH-meter (Hanna Instr.) equipped with pH combination electrodes (Ross), respectively. Standardization of pH-measurements was made against NBS buffers pH 7.413 (at 25 °C) and 9.180 (at 25 °C). Total alkalinity was analysed in the field using a hand-held titrator and 1.6 n sulfuric acid cartridges (Hach Co.). Dissolved oxygen was determined according to the Winkler method employing the same titration instrument and 0.2 n sodium thiosulfate cartridges. For the analysis of main cations, samples were filtered through glass fibre filters (Whatman GF/F, nominal pore size 0.7 µm) and preserved with HNO_3. In the laboratory cations (calcium, magnesium) were analysed by flame atomic absorption (Philips PU 9200X). Parameters of the carbonate system, partial pressure of CO_2 (pCO_2) and the saturation with respect to calcite and aragonite, were calculated with the program PHREEQE (Parkhurst et al., 1990). Saturation is given by the saturation index $SI = \log (IAP/K_{SO})$ (Stumm & Morgan, 1996) where IAP denotes the ion activity product and K_{SO} is the solubility product of the corresponding mineral (solid phase).

Stable isotope analysis of oxygen of H_2O and carbon of dissolved inorganic carbon have been carried out by Bert Kers in the laboratory of Dr. Ir. Hans van der Plicht, Centrum voor Isotopen Onderzoek, University of Groningen, the Netherlands. Samples of water were taken using 150 ml Schott glas bottles (12.06.1999). Prior to sampling, 2-3 drops $HgCl_2$ solution were added to the bottles for sterilization. Sample water was gently filled in to avoid degassing and gas bubble formation. After hermetically sealing, the bottles were keep cool in the dark and sent to the Centrum voor Isotopen Onderzoek Groningen on 15.06.1999. Stable oxygen and carbon isotope analysis of tufa carbonates were measured by Dr. Michael Joachimski, Institute of Geology, University of Erlangen, Germany.

4 WATER CHEMISTRY ALONG THE CREEK

Water chemistry data from sampling campaigns in March 1997 and June 1999 are provided in Tab. 2. The main spring waters discharge with an pH of 7.2 - 7.4 and Ca^{2+} concentrations of 1.91-2.02 mmol L^{-1}. The water is slightly undersaturated with respect to calcite and has a very high pCO_2 (8968-12903 µatm) as it is expected for karst spring waters. Waters at the tufa cascade show a pH of 7.6 -7.7. The Ca^{2+} concentrations of its small spring are higher than at the main spring. The water of the cascade is already slightly calcite supersaturated but still high in pCO_2 (3426 - 4211 µatm). Ongoing CO_2 degassing causes a pH rise by 0.1 units after spilling over the cascade. The pH of 8.3 -8.4 at the middle creek section is considerably higher than at the main spring and cascade. Ca^{2+} (2.15 - 2.44 mmol L^{-1}) is higher than that of the main spring but lower compared to cascade spring waters. Calcite supersaturation is risen to 10 to 11-fold (SI_{Cc} = 1.00 - 1.06) and pCO_2 dropped to 698-1043 µatm, that is two to three times of the atmospheric level. Lower creek waters are characterized by a pH, Ca^{2+} concentration, pCO_2, and calcite supersaturation similar to that of the middle creek section. The waters differ from middle creek waters only with regard to higher temperatures during summer.

In summary, pH rises by drop in pCO_2 along the creek, thereby rising the calcite supersaturation to values favourable

for $CaCO_3$ precipitation. Alkalinity slightly declines due to calcite precipitation. Though pCO_2 considerably drops, it does not reach an equilibrium with the atmosphere and remains two times higher than the atmospheric level of 330 µatm. Ca^{2+} and Mg^{2+} concentrations fluctuate along the creek because of several side springs that contribute to the main creek waters. Whereas most physicochemical parameters are almost constant throughout the year, a temperature rise along the creek is only evident during summer times (Wedemeyer, 1999).

5 CYANOBACTERIAL MORPHOTYPES INVOLVED IN TUFA BIOFILMS

Nine cyanobacterial morphotypes dominate the cyanobacterial biofilms in the Deinschwanger Bach. Further descriptions of microorganisms present in the Deinschwanger Bach are provided by Wedemeyer (1999).

Phormidium incrustatum (NÄG.) GOM. This morphotype is commonly described from European tufa biofilms (e.g., Fritsch, 1949, 1950; Symoens, 1957; Kann, 1973, Monty, 1976; Freytet & Plet, 1996; Freytet & Verrecchia, 1998; Janssen et al., 1999; Merz-Preiß & Riding, 1999). *Phormidium incrustatum* is a major element of biofilms that form stromatolitic crusts below the tufa cascade (Pl. 2/7) and at the middle and lower creek section of the Deinschwanger Bach (Pl. 3/5-6, 4/4-7, 6/1-3). The trichomes are straight, up to 800 µm long, and show a gliding motility on agar plates. The trichome diameter varies between 3.5 µm and 5 µm at the different sites. Few, single filaments of slightly larger diameter (7 µm) have been observed at the lower creek section. The cells are disc-shaped and 1.5-2.5 µm long and the cell walls are inserted laterally. Some filaments have been observed that show a lower frequency in cell division, so that the cells appear almost isometric. The apical cell is flat-hemispherical and rounded (Pl. 6/2). No constrictions have been observed, but concave-convex cell boundaries often occur (Pl. 6/2). The cytoplasm shows abundant inclusions (see Jensen, 1985) such as polyhedral bodies, cyanophycin granules and polyphosphate bodies (Pl. 2/8), occasionally concentrated at the cell boundaries. The peripheral parts of the cytoplasm are dark-green due to accumulation of thylakoids. The sheath of *Phormidium incrustatum* is firm, lamellated, and 0.6-0.7 µm thin (Pl. 2/8). *Phormidium incrustatum* commonly shows tufts composed of radiating erect filaments (*Ph. incrustatum* α) or densely arranged erect filaments in parallel (*Ph. incrustatum* β) (see e.g., Freytet & Plet, 1996).

Similar or identical morphotypes, in particular when showing disc-shaped cells and a distinct sheath, are occasionally assigned to *Lyngbya martensiana* Menegh. (e.g., Stirn, 1964; Scharfenberg, 1994) or *Lyngbya* sp. (Persoh, 1998). *Lyngbya calcarea* (Tilden) Symoens is regarded by Symoens (1947) as identical to *Lyngbya martensiana* Menegh. var. *carcarea* Tilden. Later, he considered *Lyngbya calcarea* to be *Phormidium incrustatum* (Symoens, 1957: 236). *Lyngbya digueti* Gom. in Stirn (1964) might represent a variety of *Phormidium incrustatum* with isometric cells. Pentecost in Merz-Preiß & Riding (1999) termed the dominant species of tufa biofilms in creeks near Bad Urach *Phormidium* (*Lyngbya*) *incrustatum*. However, it remains unclear if all these populations of *Phormidium incrustatum* belong to one phylogenetic species because analysis of 16S rRNA genes have yet not been carried out.

Phormidium foveolarum Gom. Erect filament bundles of this morphotype form dense, calcifying meadows at the top of tufa crusts taken in late summer and autumn (Pl. 5/1-5). The trichomes are straight to slightly curved and up to 70 µm long. The filaments are erect, more or less parallel, often arranged in a brush-like pattern. The trichome diameter varies between 1.3 and 1.5 µm. The cells are as long as wide (isometric) and cell boundaries slightly constricted (Pl. 5/5). Wherever the filaments are free of carbonate, a firm sheath less than 0.5 µm thin can be recognized around each trichome. Comparable morphotypes have been asigned to *Phormidium foveolarum* Gom. (e.g., Scharfenberg, 1994; Freytet & Verrecchia, 1998), which is similar to the present morphotype with regard to its filament diameter, cell shape, and filament arrangement. Janssen et al. (1999) describe *Phormidium foveolarum* together with *Phormidium incrustatum* to be a major component in tufa biofilms from Belgium.

Short, erect filaments 5 to 16 cells long, which occur in uppermost parts of tufa crusts at the tufa cascade (Pl. 2/5) and the middle creek section possibly also belong to the morphospecies *Phormidium foveolarum*. The filaments are 5-10 µm long, 1.5 µm in diameter, and are apparently attached at their basis to the substrate. The cells are isometric or slightly shorter than long. The cell boundaries are clearly constricted. The sheath is thin and only faintly visible.

Pleurocapsa minor Hansgirg. This morphotype is a common part of epilithic biofilms at the main spring of the Deinschwanger Bach (Pl. 1/2-3). It has also been found on artificial substrates that were placed only partly submerged. *Pleurocapsa minor* is composed of vertical rows of spherical to elongated cells forming a nematoparenchymatous thallus. The hemispherical to sheet-like colonies attain 130 µm thickness and several 100 µm lateral extension. The cell size ranges from 3x5 to 1x11 µm. Cell division occurs in several oblique planes and leads to false branching. The cells are separated by up to several µm wide spaces that are filled by a faintly visible exopolymer matrix (sheath). Cells at the top of the colonies often show the formation of 1-µm-sized nanocytes. *Pleurocapsa minor* is a common epilithic cyanobacterium in tufa-depositing creeks, rivers, and ponds (e.g., Geitler, 1932; Grüninger, 1965; Scharfenberg, 1994; Winsborough et al., 1994; Freytet & Plet, 1996; Freytet & Verrecchia, 1998). The morphotype is probably a collective "species" (Geitler, 1932).

Chamaesiphon subglobosus (Rostaf.) Lemmermann. Unicellular cyanobacteria that reproduce by unequal, perpendicular division, were recognized at the surface of sparitic encrustation of moss cauloids at the tufa cascade (Pl. 2/5). Initially, the cells are spherical and 1.5 µm to 2.5 µm in diameter. Epifluorescence microscopy reveals a strongly fluorescent peripheral cytoplasm and a less fluorescent, irregular centroplasm. When attached to a tufa crust surface, the initially spherical cells get elongated to form ovoid cells

sampling site	sample number	season, date	substratum	biotic community	carbonate precipitation	carbonate corrosion
main spring	RT96/II-S	summer 22.07.1996	Oxfordian limestone	*Phormidium*-encrusted, cyanobacteria		+++
	RT97/II-K	autumn 30.09.1997	Solnhofen limestone (introduced)	endolithic cyanobacteria		+++
	RT97/II-M	autumn 30.09.1997	steel iron (introduced)	*Phormidium*, mat phototrophic bacteria	-	(iron oxide/hydr.)
tufa cascade	RT99/G-a	spring 12.06.1999	bryophyta (*Cratoneurum*)	(scattered bacteria and rare coccoid and filamentous cyanobacteria)	++	+
	RT99/G-b	spring 12.06.1999	bryophyta (*Cratoneurum*)	(*Hantzschia*-rich diatoms-endolithic cyanobacterium sp. 3)		+++
	RT99/G-c	spring 12.06.1999	recent tufa crust	*Phormidium incrustatum*-endolithic cyanobacterium sp. 3	+++	++
	RT96/III-S	summer 22.07.1996	bryophyta (*Cratoneurum*)	(scattered bacteria and rare cyanobacteria)	+++	
	RT96/III-F	autumn 01.10.1996	bryophyta (*Cratoneurum*)	(scattered bacteria and rare cyanobacteria)	+++	
	RT97/III-K	autumn 30.09.1997	Solnhofen limestone (introduced)	*Phormidium*-endolithic cyanobacteria/fungi		+++
	RT97/III-H	autumn 30.09.1997	wood (introduced)	fungi and mat phototrophic bacteria	+	
	RT97/III-20	winter 01.03.1997	bryophyta (*Cratoneurum*)	(scattered bacteria and rare cyanobacteria)	+?	
middle creek section	RT96/IV-F	spring 01.05.1996	bryophyta (*Rhynchostegium*)	*Fb. intermedium*, *Fb. intermedium* (deeper parts diatoms)	++	
	RT99/B-a	spring 12.06.1999	subfossil tufa crust	*Fb. intermedium* (deeper parts cocoid cyanobacteria basally *Hantzschia amphioxys*)	++	++
	RT99/B-b	spring 12.06.1999	subfossil tufa crust	*Fb. intermedium* (basally *Hantzschia amphioxys*)	++	++
	RT96/IV-1	summer 22.07.1996	bryophyta (*Rhynchostegium*)	*Fb. intermedium* (deeper parts *Fb. intermedium*, diatoms)	++	
	RT97/IV-K	autumn 30.09.1997	Solnhofen limestone (introduced)	*Fb. intermedium*, *Fb. brevifolium* (basally endolithic cyanobacteria)	++	++
	RT97/IV-20	winter 01.03.1997	bryophyta (*Rhynchostegium*)	(scattered bacteria, *Fb. intermedium*, coccoid cyanobacteria)	+?	
lower creek section	RT96/I-F	spring 01.05.1996	chlorophyta (*Schizophora*)	diatoms (and rare *Fb. intermedium*)	+	
	RT99/F	spring 12.06.1999	Oxfordian limestone	*Fb. intermedium*, *Fb. brevifolium* (deeper parts diatoms, *Fb. intermedium*)	+++	+
	RT96/I-2 (A)	summer 22.07.1996	subfossil tufa crust	*Fb. intermedium*, *Fb. brevifolium*, diatoms (basally endolithic cyanobacterium sp. 2)	+++	++
	RT96/I-1	summer 22.07.1996	bryophyta (*Rhynchostegium*)	*Fb. intermedium*, *Fb. intermedium* (deeper parts diatoms, *Fb. intermedium*)	+++	
	RT96/I-2	summer 22.07.1996	subfossil tufa crust on Oxfordian limestone	*Fb. intermedium*, *Fb. brevifolium* (deeper parts diatoms, *Fb. intermedium*, basally endolithic cyanobacteria)	+++	+
	RT96/I-5	summer 22.07.1996	bryophyta (*Rhynchostegium*)	*Fb. intermedium*, *Fb. brevifolium* (deeper parts diatoms, *Fb. intermedium*)	+++	
	RT97/I-H	autumn 30.09.1997	wood (introduced)	*Fb. brevifolium*, *Fb. intermedium* (deeper parts diatoms)	+++	
	RT97/I-M	autumn 30.09.1997	steel iron (introduced)	*Fb. intermedium*, *Fb. intermedium* (deeper parts diatoms)	+++	(iron oxide/hydr.)
	RT97/I-P	autumn 30.09.1997	polystyrene (introduced)	*Fb. intermedium*, *Fb. intermedium* (deeper parts diatoms)	+++	
	RT97/I-K	autumn 30.09.1997	Solnhofen limestone (introduced)	*Fb. brevifolium*, *Fb. intermedium* (deeper parts diatoms, basally *Hantzschia amphioxys*)	++	++
	RT96/I-10	autumn 22.11.1996	bryophyta (*Rhynchostegium*)	*Fb. intermedium*, *Fb. brevifolium*, diatoms (deeper parts *Fb. intermedium*, diatoms)	+++	
	RT96/I-11	autumn 22.11.1996	chlorophyta (*Schizophyta*)	*Fb. intermedium*, *Fb. brevifolium*, diatoms (deeper parts diatoms)	++	+
	RT97/I-W (A/15a)	winter 01.03.1997	Oxfordian limestone	diatoms (rare *Fb. intermedium*)	+?	
	RT97/I-W (A/15b)	winter 01.03.1997	Oxfordian limestone	diatoms (rare *Fb. intermedium*) (deeper parts *Fb. intermedium*, *Fb. brevifolium*, basally *Hantzschia*)	+?	
	RT97/I-W (A/15c)	winter 01.03.1997	chlorophyta (*Schizophyta*)	diatoms (deeper parts *Fb. intermedium*, *Fb. brevifolium*)	+?	
	RT97/I-20	winter 01.03.1997	chlorophyta (*Schizophyta*)	diatoms	+?	

Tab. 1. Investigated biofilm samples of the Deinschwanger Bach. Carbonate precipitation/corrosion based on observations in biofilm sections is indicated as "not observed" (-), "present" (+), "moderate" (++), and "strong" (+++).

Sample	T °C	pH	EC µS cm^{-1}	Eh mV	O_2 mmol L^{-1}	Tot Alk meq L^{-1}	Ca mmol L^{-1}	Mg mmol L^{-1}	SI_{Ar}	SI_{Cc}	pCO_2 µatm
Sampling period March 1997											
spring	8.8	7.21	525	280	0.234	4.42	2.02	1.06	-0.33	-0.17	12903
cascade	7.3	7.60	480	180	0.281	3.70	2.77	0.15	0.20	0.36	3426
creek station 1	8.3	8.44	502	150	0.293	4.22	2.44	0.57	0.91	1.06	698
creek station 2	7.7	8.44	500	140	0.344	4.21	2.39	0.57	0.89	1.04	712
Sampling period June 1999											
spring	8.8	7.41	546			4.86	1.91	1.20	-0.10	0.06	8968
cascade	8.2	7.71	562			4.60	2.94	0.14	0.36	0.51	4211
creek station 1	9.6	8.32	533			4.72	2.15	0.84	0.84	1.00	1043
creek station 2	10.4	8.43	531			4.54	2.05	0.82	0.92	1.08	778

Tab. 2. Water chemistry data of spring and creek water of the Deinschwanger Bach. EC: electrical conductivity. Saturation index SI is given on logarithmic scale, which means saturation is reached at SI = 0, and SI = 1 denotes a 10-fold supersaturation (W). Ar: Aragonite, Cc: Calcite.

1.9 x 2.6 µm to 3.7 x 6.2 µm in size. Each of these "sporangia" releases a single exocyte of 1.5 µm diameter at its apical pole (Pl. 2/5). *Chamaesiphon* is attached to the substratum by a thin sheath, which is open at its apical side. The present species morphologically fits to *Chamaesiphon subglobosus* as described in Geitler (1932: 428 f.). Spherical to ovoid cells of the same size and internal structure also occur within pore spaces of tufa crust at the cascade and at the middle creek section (Pl. 2/6, 3/7). They are considered to represent a different ecomorphotype of the same *Chamaesiphon* species. Located within the subsurface voids of the crusts, these cells show an elongation which is followed by a simple binary fission.

Aphanocapsa sp. Coccoid cyanobacteria which form loose aggregates of up to more than 50 cells have been observed in voids of sparitic moss encrustations at the investigated small tufa cascade (Pl. 2/6). The cells are spherical (1.2 µm diameter) to slightly ovoid (1.2 x 2.1 µm) and show a binary fission. No defined arrangement of cells occurs due to irregularly oriented fission planes. The cells and their diffluent sheaths remain uncalcified. A morphologically comparative species is *Aphanocapsa endolithica* Ercegovic, which might be endolithic or chasmolithic (see Geitler, 1932: 155).

Hyella fontana Huber & Jadin. Endolithic cyanobacteria of the *Hyella* morphotype are present at almost all submerged or temporarily submerged limestone substrates (Pl. 1/4-5, 3/8, 4/3). Strikingly, they also occur within presently growing tufa crusts, thereby contributing to the high porosity (Pl. 5/1-2). *Hyella* colonies on dense, fossil limestones show a near-surface part composed of 10-20 coccoid cells (often "status chroococcoides"). The cells of this part are 1-8 µm in diameter and show a multiple fission pattern. Downwards penetrating pseudofilaments are bi- or triserial at first, uniserial at the distal tips. The cell diameter averages 4 µm. Branches develop from protuberances near the end of the elongated cells so that the cells appear L-shaped. *Hyella* borings reach up to 230 µm deep into the substrates. *Hyella* specimen within tufa crusts are less regular developed and show radial developed pseudofilaments. *Hyella fontana*

Plate 1 Corrosive biofilms of the main spring of the Deinschwanger Bach, Bavaria.

Fig. 1. Field view of the main spring (site 1). Arrow points to limestone cobbles covered by greenish-grey biofilms shown in Pl. 1/2-3. November 1996.

Fig. 2. Coccoid cyanobacteria (*Pleurocapsa minor*; pleu) and filamentous green algae (*Gongrosira* sp.; gongr) are the main components of epilithic biofilms on limestone cobbles at the main spring of the Deinschwanger Bach (site 1). Summer (22.07.1996). Epifluorescence micrograph (ex 450-490 nm, em 520-575 nm). Sample RT 96/II-5A.

Fig. 3. Overview of epilithic and endolithic biofilm parts on a limestone cobble at the main spring. Epilithic parts are mainly formed by *Pleurocapsa minor* (pleu) and *Gongrosira* sp. (gongr). Straight vertical borings (arrow) substantially corrode the substrate rock. No calcite precipitates form within the undersaturated spring water. Main spring of Deinschwanger Bach (site 1). Summer (22.07.1996). Overlay of Nomarski optics and epifluorescence micrograph (ex 450-490 nm, em 520-575 nm). Sample RT 96/II-5A.

Fig. 4. Top of substrate plate (Solnhofen limestone) placed at the main spring of the Deinschwanger Bach (site 1) for 10 months. Autumn (30.09.1997). Plane polarized light. Sample RT 97/II-K.

Fig. 5. Epifluorescence micrograph of the frame shown in Pl. 1/4. The top of the limestone substrate is strongly affected by the endolithic cyanobacterium *Hyella fontana*. Projection of 33 confocal laser scanning micrographs (ex 488 nm, em >505 nm, pinhole 99 µm).

Fig. 6. Bottom of an artificial substrate (Solnhofen limestone) placed for 10 months at the main spring of the Deinschwanger Bach (site 1). Autumn (30.09.1997). Plane polarized light. Sample RT 97/II-K.

Fig. 7. Epifluorescence micrograph of the same view shown in Pl. 1/6. Straight borings of the endolithic cyanobacterium 1 perforate the limestone. Epifluorescence micrograph (ex 450-490 nm, em 520-575 nm). For scale see Pl. 1/6.


spring
orifice
1

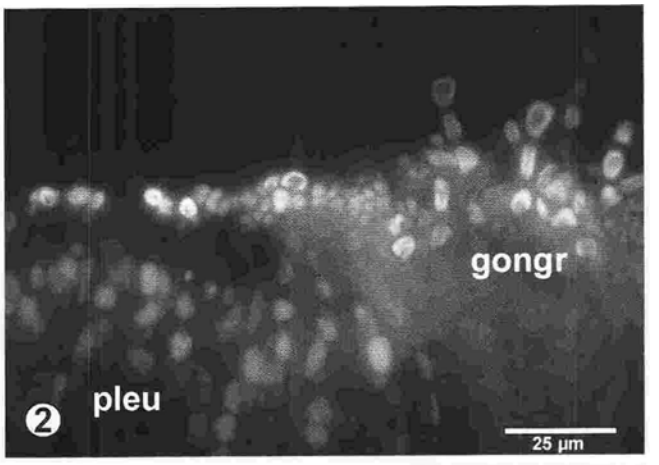
gongr
pleu
2
25 µm

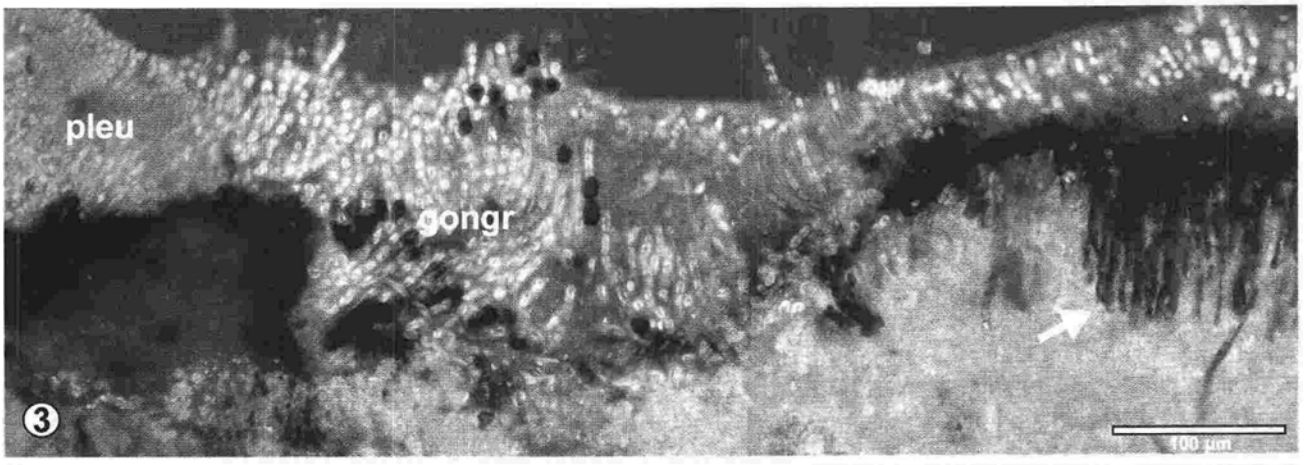
pleu
gongr
3
100 µm

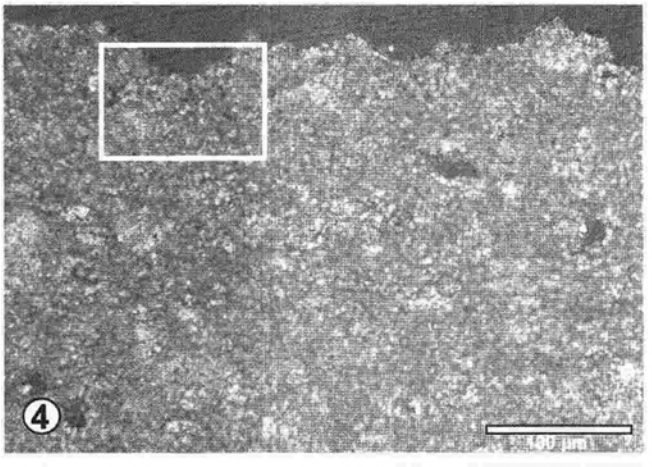
4
100 µm


5
10 µm

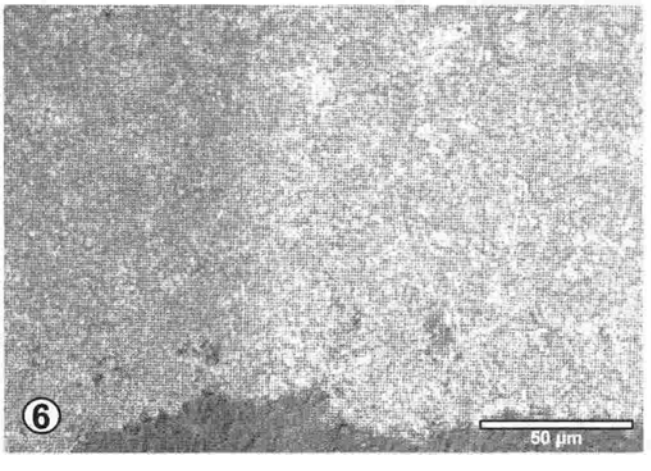
6
50 µm

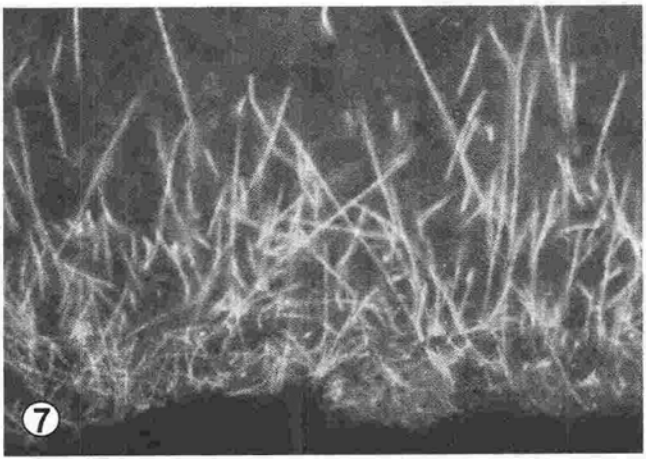
7

Huber & Jadin (see Geitler, 1932: 372 f.), which is known to occur in tufa systems (e.g., Freytet & Verrecchia, 1998), closely fits to this description. Similar morphotypes have also been assigned to *Pleurocapsa minor* (e.g., Rott, 1994).

Endolithic cyanobacterium 1. The straight borings of endolithic filaments poor in characteristics occur on the lower side of limestone substrates (Pl. 1/6-7). The trichomes are 3 µm in diameter. Two observations of possible false branching have been made. The cells are 3 - 6 µm long and show one to three non-fluorescent inclusions.

Endolithic cyanobacterium 2: The trichomes are 1.3 - 1.7 µm in diameter. The cells are isometric, 2-6 µm long. The cell boundaries are not constricted. The borings attain up to 225 µm depth. The present endolithic filamentous cyanobacterium occurs on shaded undersides of limestone substrates, which commonly lack *Hyella*. The same filaments that occur on the upper side of limestone substrates together with *Hyella* are irregularly curved.

Endolithic cyanobacterium 3. Cyanobacterial borings similar to the endolithic cyanobacterium 2, but of slightly smaller diameter (1.2 µm), have been found to corrode microspar crusts at the tufa cascade (Pl. 2/5). The cells are 2-5 µm long and slightly constricted at their cell walls. Occasionally, false branching occurs. Marginal parts of the cell plasma are strongly fluorescent (thylakoids), whereas the centroplasm is far less fluorescent. Because of structural differences of the cytoplasm, the endolithic cyanobacterium 3 is considered as a separate species. A morphologically comparable species is *Schizothrix perforans* (Ercegovic) Geitler, which is of the same dimensions, endolithic, and shows constrictions at its cell boundaries. According to the recent traditional-botanic revision *Schizothrix perforans* (Ercegovic) Geitler is placed in the new genus *Leptolyngbya* (Anagnostidis & Komárek, 1988).

6 COMPOSITION, STRUCTURE, AND CALCIFICATION PATTERNS OF BIOFILMS

6.1 Main spring

Rounded and subangular limestone cobbles at the main spring of the Deinschwanger reeks are veneered by greenish-grey biofilms (Pl. 1/1). Dark-green covered projections consist of the substrate limestone and probably represent dissolution remnants. No $CaCO_3$ precipitates have been observed.

Biofilms consist of an endolithic and a thin epilithic part (Pl. 1/2-3). The uppermost 100 µm of the limestone cobbles are intersected by a dense network of endolithic filaments. *Hyella* with pseudofilaments up to 100 µm length is the dominant endolith in most places. In addition, some places

Plate 2 Biofilms and $CaCO_3$ precipitates of the tufa cascade, Deinschwanger Bach, Bavaria.

Fig. 1. Field view of the small tufa cascade at the southern side of the Rohrenstadt Valley, June 1999. The green bryophyte cushions (*Crateroneuron commutatum*) are calcite-encrusted at their water-soaked base. Arrow indicates position of sample shown in Pl. 2/2 and Pl. 2/3. The photo covers an area approximately 5 m wide.

Fig. 2. Longitudinal section of a moss cauloid taken from the small tufa cascade shown in Pl. 2/1. The bryophyte surfaces are covered by euhedral rhombs of calcite. Spring (01.05.1996), tufa cascade (site 2), Rohrenstadt Valley. Transmitted light. Sample RT 96/III-F.

Fig. 3. Detail of euhedral rhombs growing upon phylloids of a bryophyte. Note that the phylloid surfaces are free of biofilms. Spring (01.05.1996), tufa cascade (site 2), Rohrenstadt Valley. Nomarski optics. Sample RT 96/III-F.

Fig. 4. Fruiting body of a ascomycete fungus growing on a wood substrate that has been placed for 10 month in front of the cascade. Note microspar crystals and tiny micrite crystals that have formed at the surface of the fungus (insert). Autumn (30.09.1997), tufa cascade (site 2), Rohrenstadt Valley. Nomarski optics. Sample RT 97/III-H.

Fig. 5. Epilithic biofilm of *Chamaesiphon subglobosus* (chamae; note exocyte formation) and short filamentous cyanobacteria (sfc). The numerous filaments below are of endolithic origin (endolithic cyanobacterium 3: endo). Spring (12.06.1999), tufa cascade (site 2), Rohrenstadt Valley. Deconvolved epifluorescence micrograph (ex 450-490 nm, em 520-575 nm). Sample RT 99/G-b.

Fig. 6. Colonies of the coccoid cyanobacterium *Aphanocapsa* sp. (aphano) in voids between spar crystals of moss encrustations at the tufa cascade. Cells of *Chamaesiphon subglobosus* (chamae) are also present, but do not produce exocytes within the void. Spring (12.06.1999), tufa cascade (site 2), Rohrenstadt Valley. Deconvolved epifluorescence micrograph (ex 450-490 nm, em 520-575 nm). Sample RT 99/G-b.

Fig. 7. Stromatolitic tufa crusts 5 m downstream of the cascade consist of microsparitic tubes of *Phormidium incrustatum*. Spring (12.06.1999), below tufa cascade (site 2), Rohrenstadt Valley. Overlay of transmitted light and epifluorescence micrograph (ex 450-490 nm, em 520-575 nm). Sample RT 99/G-c.

Fig. 8. Longitudinal section of the cyanobacterium *Phormidium incrustatum* showing filamentous microorganisms within the sheath-surrounding exopolymer matrix. Cyanobacterial cell inclusions comprise thylacoid membranes, dark polyhedral bodies (carboxysomes; cb), and light polyphosphate bodies (pp). Note lamellate structure of the sheath (sh). Autumn (30.09.1997). TEM micrograph #6769. Sample RT97/Vb.

Fig. 9. Decayed trichome of *Phormidium incrustatum*, internally colonized by numerous filamentous and rod-shaped heterotrophic bacteria. Autumn (30.09.1997). TEM micrograph #6766. Sample RT97/Vb.

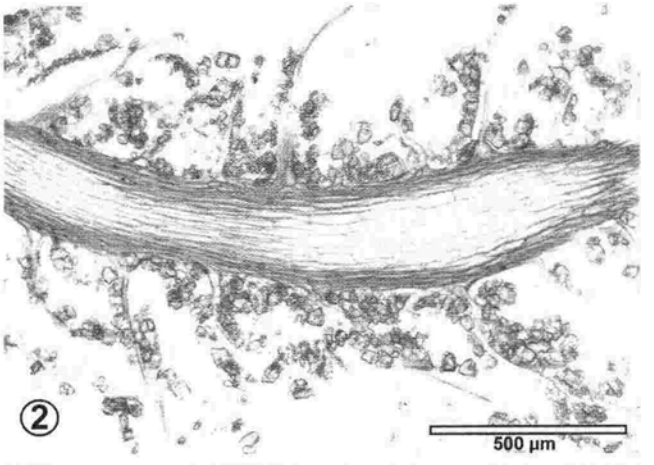
500 µm

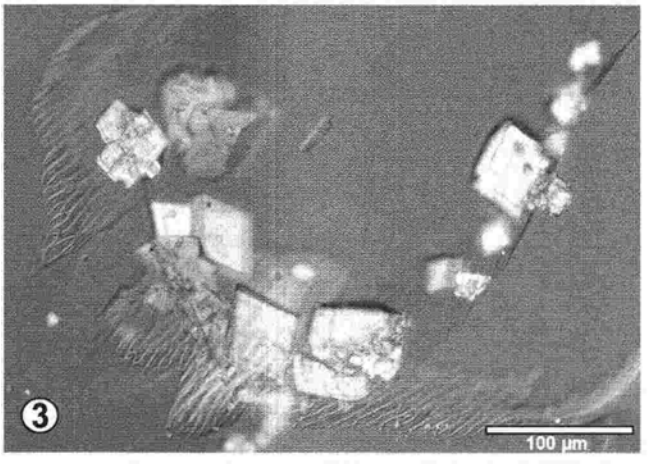
100 µm

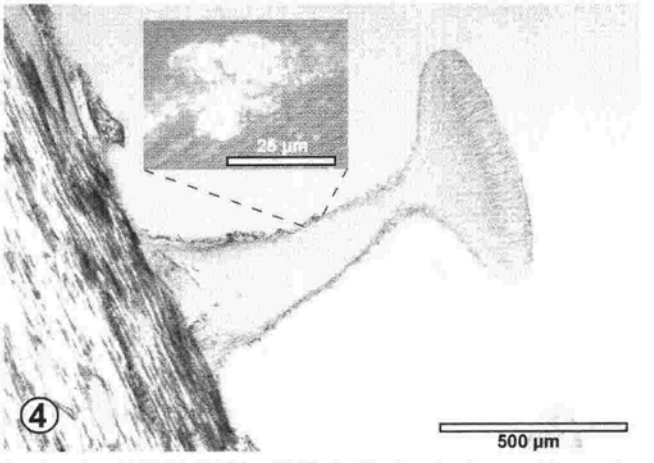
25 µm
500 µm

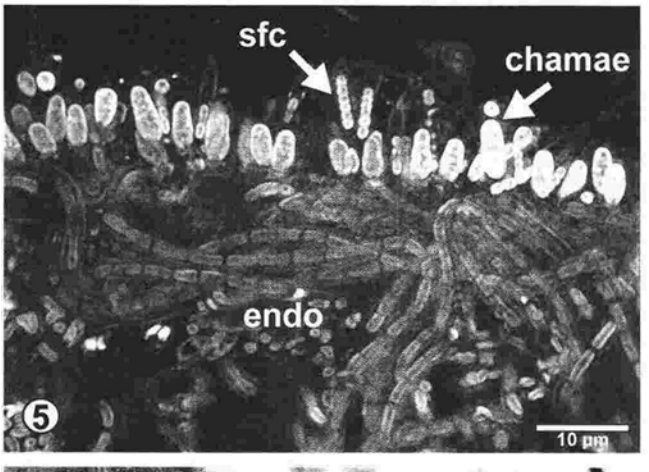
sfc
chamae
endo
10 µm

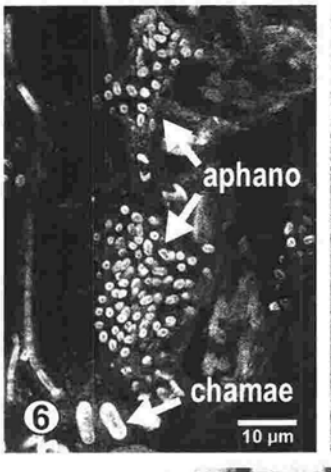
aphano
chamae
10 µm


100 µm

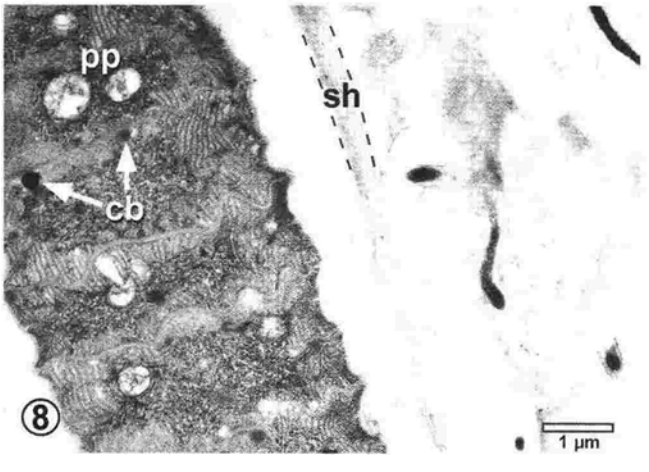
pp
sh
cb
1 µm

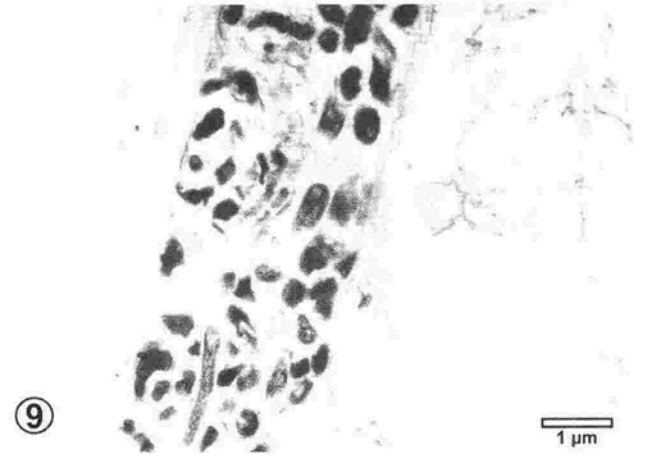
1 µm

show dense vertical borings of 100 µm depth (occasionally up to 1.2 mm depth) that represent borings of the green alga *Gongrosira* (Pl. 1/3). Numerous thin, irregularly arranged filaments of the endolithic cyanobacteria 1 and 2 occur, too. Cell-walls of green algae and cyanobacterial sheaths are often dark-brown pigmented (Pl. 1/3). The epilithic part of the biofilm is 50-120 µm thick and only patchy developed. It consists mainly of the green alga *Gongrosira* and the coccoid cyanobacterium *Pleurocapsa minor*, which forms a cushion-like to continuous layer (Pl. 1/2-3). Locally, thin erect cyanobacterial filaments (1.5 µm diameter, cells up to 10 µm long) occur as well.

The Solnhofen limestone plate placed at the spring shows on its upper side a similar biofilm with intensively developed endolithic borings (*Hyella* and thin borings of the endolithic cyanobacteria 1 and 2) (Pl. 1/4-5). The epilithic part is only poorly developed, consisting of scattered, small *Pleurocapsa* colonies. The lower, shaded substrate side lacks *Hyella* but is affected by straight borings of the endolithic cyanobacteria 1 (Pl. 1/6-7).

6.2 Tufa cascade

Samples have been taken immediately at the beginning of the cascade, at central parts of the cascade (Pl. 2/2), and at the steep flow-off 5 m downstream of the cascade. Unfortunately, it was not possible to place artificial substrates properly at the cascade itself. Instead, the substrates were placed immediately in front of the cascade, though only insufficiently submerged in the water flow. The Solnhofen limestone substrate was affected by endolithic biofilms similar to that of the main spring, whereas the wood substrate was colonized by ascomycete fungi (Pl. 2/4). Strikingly, some hypidiomorphic and idiomorphic calcite crystals were observed attached to the fruiting bodies.

At the beginning of the cascade, moss cauloids (*Craterneurum*) are covered by 275-500 µm thick sparitic crusts composed of hypidiomorphic crystals 20-100 µm in size. These crusts are superficially heavily colonized by small diatoms (3 x 8 µm in size), green algae, cyanobacteria, and non-phototrophic bacteria. The spar crystals are densely intersected by filaments of the endolithic cyanobacterium 3 (Pl. 2/5). Voids between the crystals show patches of coccoid cyanobacteria (*Aphanocapsa*, *Chamaesiphon*) and rod-shaped bacteria, whereas the crust surface is colonized by diatoms, green algae, *Chamaesiphon* (Pl. 2/5), short filamentous cyanobacteria, and rare *Phormidium incrustatum*. All microorganisms remain uncalcified.

Moss cushions within the spilling water of the cascade (Pl. 2/1) are almost free of extensive biofilms. Only scattered filamentous cyanobacteria (*Phormidium* sp.), coccoid non-phototrophic bacteria, and fungal hyphae have been found attached to the moss phylloids. Middle and lower parts of moss phylloids are moderately to heavily calcite veneered (Pl. 2/2). The thickness of these encrustation locally exceeds 250 µm. The precipitated calcite is exclusively formed by euhedral rhombs directly attached to the moss cauloid cuticle (Pl. 2/3), which is devoid of light-optically detectable bacteria. The rhombs attain 10 to 70 µm in size. Hypidiomorphic crystals have only been found at the very rare places of epiphytic microorganisms. Only at the lower part of the tufa cascade biofilms cover the spar-encrusted moss cauloids. *Chamaesiphon* sp., *Aphanocapsa* sp. and thin filamentous cyanobacteria are abundant, but remain

Plate 3 Biofilms and $CaCO_3$ precipitates of the middle creek site, Deinschwanger Bach, Bavaria.

Fig. 1. Field view of the middle creek site showing a barrier covered by weakly calcified, submerged bryophytes (*Rhynchstegium riparioides*). Arrow points to site of sample shown in Pl. 3/2-4. Middle creek site (site 3), Deinschwanger Bach, March 1997. The photo covers an area approximately 5 m wide.

Fig. 2. Oblique section of a moss cauloid showing irregular, microsparitic calcite encrustation. Winter (01.03.1997), middle creek site (site 3), Deinschwanger Bach. Nomarski optics. Sample RT 97/IV-20A.

Fig. 3. Detail from Pl. 3/2 showing microspar upon a moss phylloid. Middle creek site (site 3), Deinschwanger Bach. Nomarski optics.

Fig. 4. Same view as in Pl. 3/3. Epifluorescence reveals numerous filamentous cyanobacteria and diatoms (arrows) at and within the irregular microspar crust. Epifluorescence micrograph (ex 450-490 nm, em 520-575 nm). For scale see Pl. 3/3.

Fig. 5. Recent carbonate crust upon subfossil tufa cobble shows tufts of carbonate tubes, which formed externally upon the sheaths of *Phormidium incrustatum*. Spring (12.06.1999), middle creek site (site 3), Deinschwanger Bach. Transmitted light. Sample RT 99/B-b.

Fig. 6. Same view as in Pl. 3/5 to show the living trichomes of *Phormidium incrustatum*. Epifluorescence micrograph (ex 450-490 nm, em 520-575 nm).

Fig. 7. Large rod-shaped cells of the coccoid cyanobacterium *Chamaesiphon subglobosus*. Within voids of tufa crusts *Chamaesiphon* does not form exocytes and divides by a simple binary fission. Spring (12.06.1999), middle creek site (site 3), Deinschwanger Bach. Deconvolved epifluorescence micrograph (ex 450-490 nm, em 520-575 nm). Sample RT 99/B-b.

Fig. 8. The contact of recent tufa crusts to subfossil carbonates is marked by a layer of the endolithic cyanobacterium *Hyella* (hy). Note filaments of the green alga *Gongrosira* (gongr) and the cyanobacterium *Phormidium incrustatum* (Ph. incr) in the newly formed crust. Spring (12.06.1996), middle creek site (site 3), Deinschwanger Bach. Epifluorescence micrograph (ex 450-490 nm, em 520-575 nm). Sample RT 99/B-b.

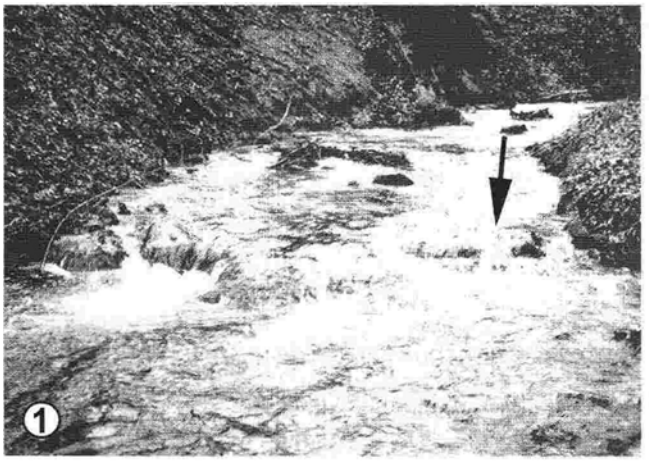

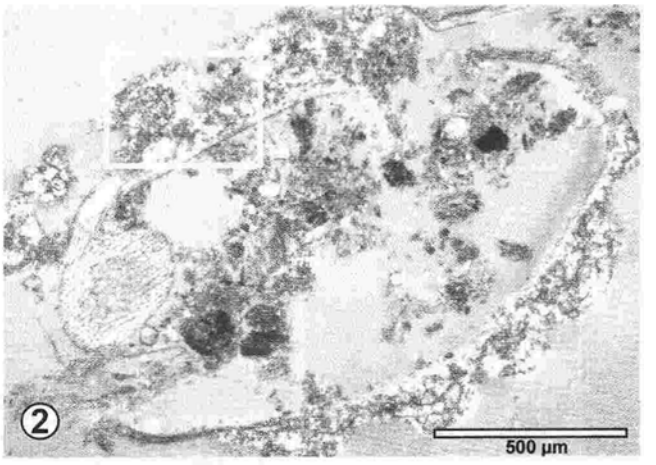
500 µm

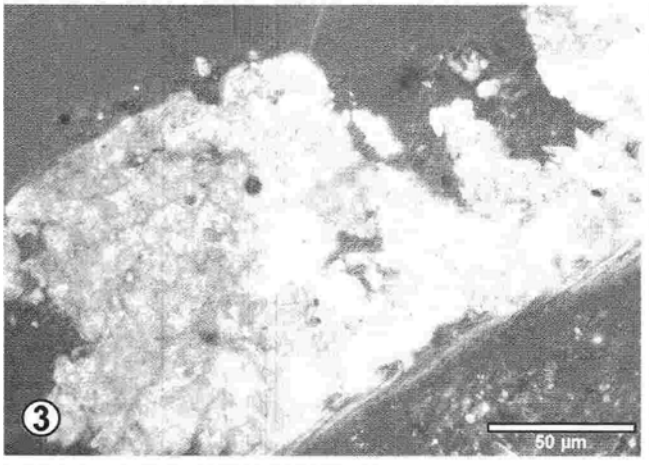
50 µm

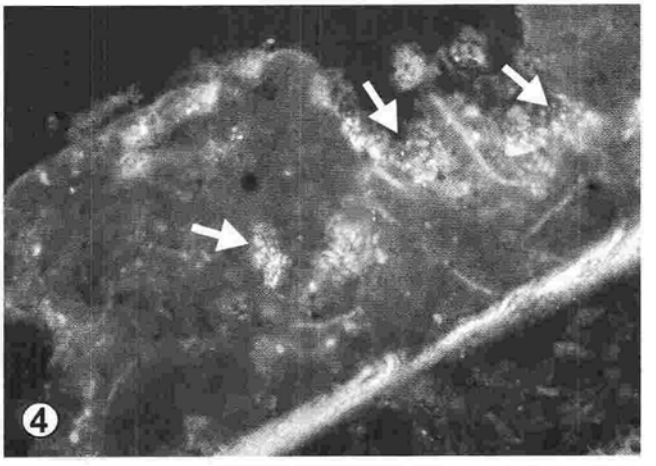

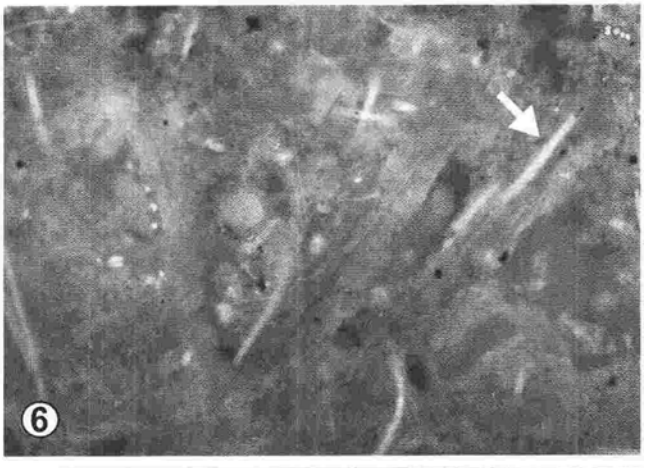

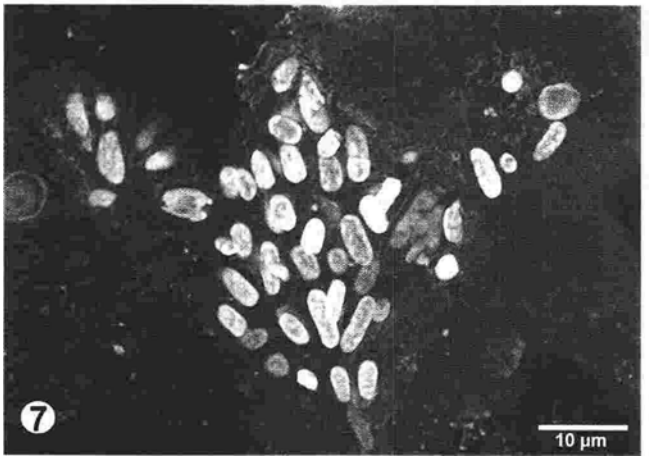
10 µm

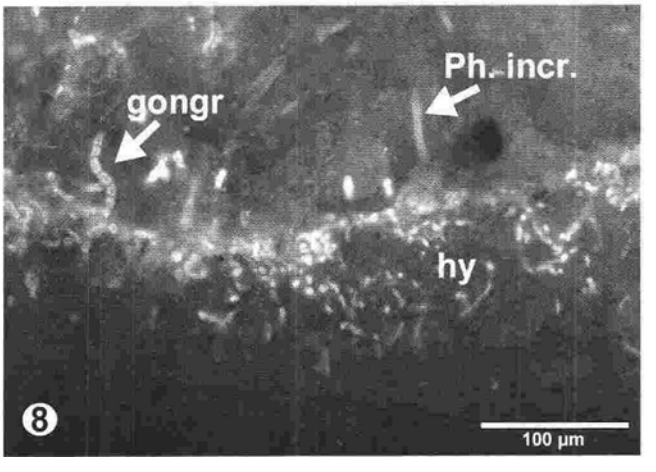
gongr
Ph. incr.
hy
100 µm

uncalcified (Pl. 2/5). Numerous borings of the endolithic cyanobacterium 3 perforate the spar crystals covering the moss cauloids (Pl. 2/5).

Blue-green coloured tufa crusts of the moss-free flow-off below the cascade are stromatolitic. The lamination is caused by an alternation in porosity of the microspar framework. Light laminae are 70-500 µm thick and show many voids and pores between the 5-10 µm sized crystals, whereas the 100-150 µm thick dark laminae show densely arranged microspar crystals of the same size. The biofilm community is dominated by erect filaments of *Phormidium incrustatum* (Pl. 2/7), which are externally mineralized by microspar, thereby forming major parts of light and dark laminae. The primary formed microspar framework is subsequently perforated by the endolithic cyanobacterium 3, which occur from top of the crusts to at least 500 µm depth. Porosity of the dark laminae is thereby increased so that the lamination locally gets less clear and faint (Pl. 2/7). Filamentous microorganisms occur within the mucilaginous matrix of the biofilm (Pl. 2/8), whereas rod-shaped heterotrophic bacteria rapidly colonize the interior of cyanobacterial trichomes upon their death (Pl. 2/9).

6.3 Middle creek section

The submerged, trailing moss cauloids (*Rhynchostegium*) of the small barrier in the creek (Pl. 3/1) are slightly to moderately calcite encrusted at their basis (Pl. 3/2). In contrast to mosses of the cascade tufa, grey-greenish biofilms are well developed. Encrustations are formed by micrite and hypidiomorphic spar crystals. The up to 200 µm thick $CaCO_3$ encrustations are discontinuous and often enclose filaments of *Phormidium incrustatum*, coccoid cyanobacteria, and pennate diatoms (Pl. 3/3-4). At places of abundant diatoms, the moss surfaces remain almost free of precipitates.

Dark-green crusts on subfossil tufa cobbles occur in front of the creek barrier. The present encrustation is 1.5 - 3 mm thick and constructed by erect bushes of microspar tubes (Pl. 3/5) which result from externally mineralized *Phormidium incrustatum* filaments (Pl. 3/6). Accessory elements are the green alga *Gongrosira* (Pl. 3/8), small diatoms, and patchy colonies of *Chamaesiphon* (Pl. 3/7). The light-dark lamination again reflects changes in porosity of the microspar framework at constant crystal sizes. The basal contact to the subfossil tufa substrate is marked by a layer of the endolithic *Hyella* (Pl. 3/8). Further, the endolithic cyanobacterium 3 corrodes the subfossil tufa in places where *Hyella* is rare or absent.

6.4 Lower creek section

Most extensive carbonate encrustations of recent age have been found at the sun-exposed lower creek section (Pl. 4/1). Submerged, trailing mosses (*Rhynchostegium*) and limestone cobbles within the creek are continuously covered by up to 5 mm thick tufa crusts (Pl. 4/2). Only the uppermost, green tips of the moss cauloids remain essentially free of $CaCO_3$. Filamentous green algal tufts (*Cladophora*) are veneered by thin microspar crusts and organic detritus, but do not form rigid, permanent deposits. Further, artificial substrates (limestone, polystyrene, wood, iron) placed in the

Plate 4 Biofilms and $CaCO_3$ precipitates of the lower creek site, Deinschwanger Bach, Bavaria.

Fig. 1. Field view of sampling site 4 at the lower creek section, March 1997. Arrow indicates the place of sampling.

Fig. 2. Oblique section of a tufa-encrusted moss cauloid (M). Arrows point to carbonate tubes that have formed around *Phormidium incrustatum* filaments. Autumn (22.11.1996), lower creek section (site 4), Deinschwanger Bach. Transmitted light. Sample RT 96/I-10.

Fig. 3. Surface of an Oxfodian limestone cobble bored by the endolithic cyanobacterium *Hyella fontana* at the basis of a tufa biofilm crust. The following tufa crust starts with a porous microspar crust (spring layer) with small diatoms, non-phototrophic bacteria and empty *Phormidium* sheaths. Late spring (12.06.1999), lower creek section (site 4), Deinschwanger Bach. Epifluorescence micrograph (ex 450-490 nm, em 520-575 nm). Sample RT 99/F.

Fig. 4. Surface part of a tufa biofilm crust sampled in late spring (12.06.1999). This porous layer shows upwards growing and tangeled *Phormidium incrustatum* filaments. Lower creek section (site 4), Deinschwanger Bach. Epifluorescence micrograph (ex 450-490 nm, em 520-575 nm). Sample RT 99/F.

Fig. 5. Same view as in Pl. 4/4 showing loosely distributed microspar aggregates between the *Phormidium incrustatum* filaments. Crossed Nicols. For scale see Pl. 4/4.

Fig. 6. Surface part of a tufa biofilm crust sampled in summer (22.07.1996). The biofilm top shows bush-like arrays of erect *Phormidium incrustatum* filaments, accompanied by *Ph. foveolarum*. Lower creek section (site 4), Deinschwanger Bach. Epifluorescence micrograph (ex 450-490 nm, em 520-575 nm). Sample RT96/I-1.

Fig. 7. Same view as in Pl. 4/6 showing dark, micritic encrustations of the bush-like filament arrays of *Phormidium incrustatum*. Lower creek section (site 4), Deinschwanger Bach. Nomarski optics.

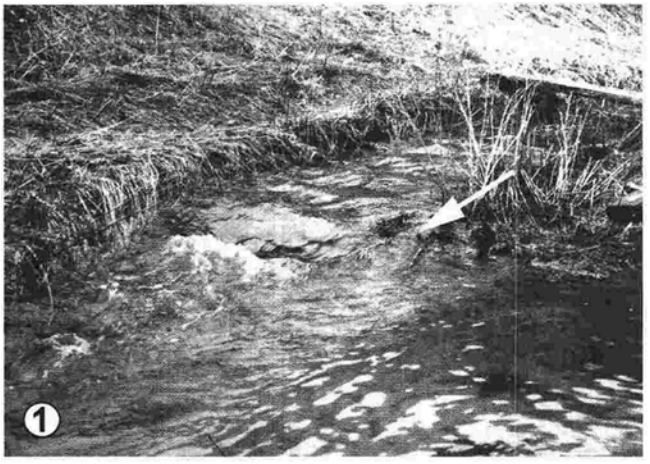

1

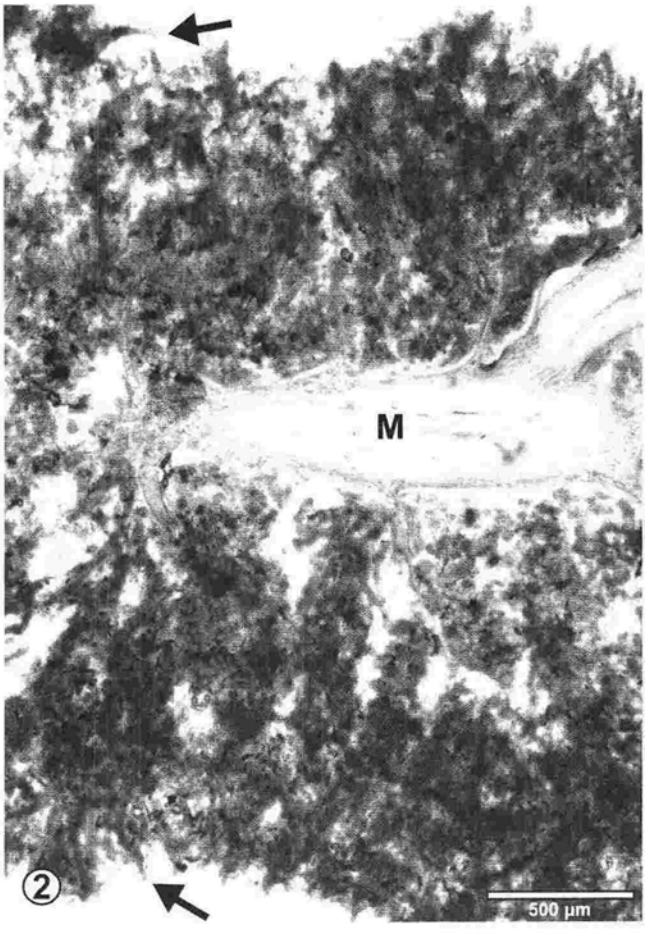

2

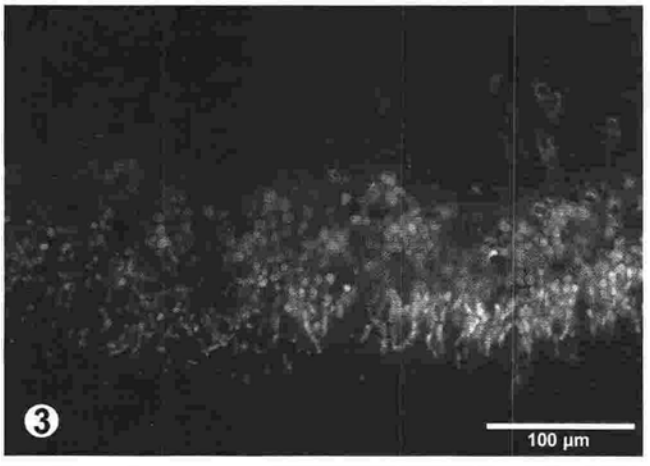

3

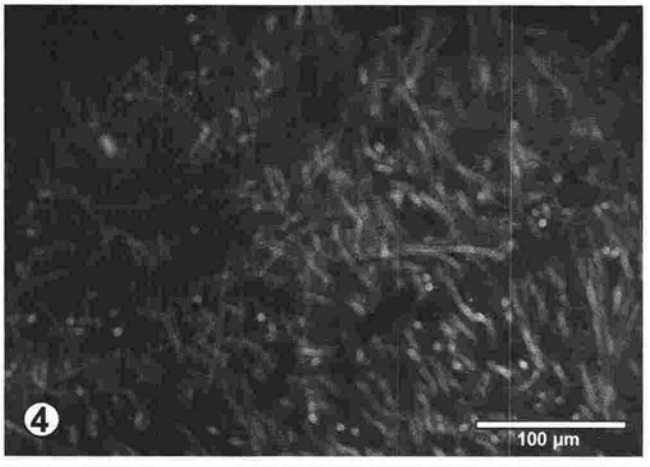

4

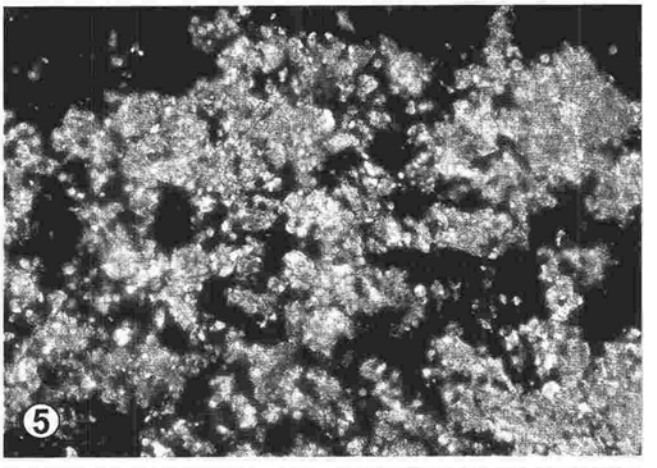

5

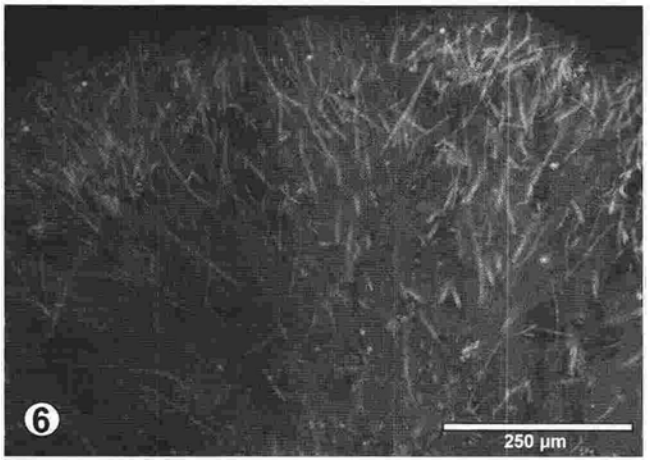

6

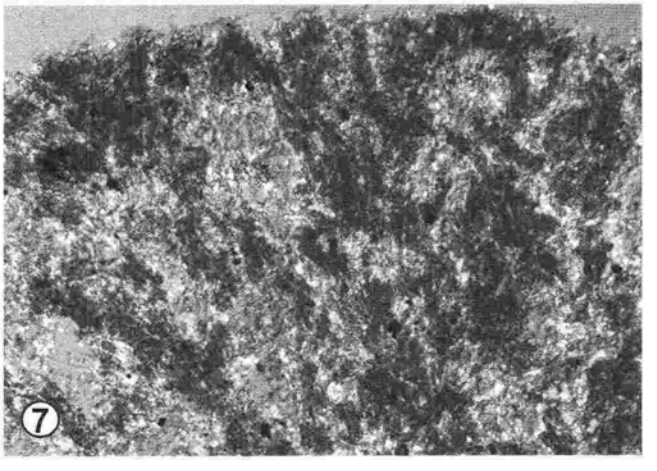

7

creek were covered by up to 1.5 mm thick tufa crusts within 10 months (22.11.96 - 30.09.97). Dominating microorganisms are the cyanobacteria *Phormidium incrustatum*, *Phormidium foveolarum*, *Hyella fontana*, and small pennate diatoms.

When developed on limestone substrates (Jurassic limestone cobbles, subfossil tufa, artifically introduced Solnhofen limestone) the tufa crust biofilms exhibit a basal endolithic zone (Pl. 4/3). The endolithic zone is largely formed by the cyanobacterium *Hyella* and additional thin borings of unknown origin. The borings are up to 100 µm deep. Though *Hyella* is most abundant at the crust base, it occurs throughout the tufa crust and contributes to the maintenance of high porosity of the constructive crust parts (Pl. 5/1-2).

The following tufa crust is characterized by up to 3 alternations of porous microsparitic layers and more dense micritic layers as a result of seasonal changes in biofilm composition and structure. However, small-scale lateral variations in biofilm composition and structure complicate the picture and continuous layers are rather the exception.

Samples taken in spring (01.05.1996; 12.06.1997) show the development of bush-like arrays of erect *Phormidium incrustatum* filaments ("*Ph. incrustatum* α") (Pl. 4/4), accompagnied by less abundant *Phormidium foveolarum*. The intensity of calcification varies laterally and vertically. Locally, only scattered hypidiomorphic microspar crystals and crystal aggregates of 5-30 µm size forming a loose, irregular, highly porous fabric (Pl. 4/4-5) between the radiating filaments. At other places, radiating filaments are externally completely covered by microspar to form calcified tufts. In general, microspar precipitates and tubular encrustations increase towards the top. Occasionaly, the layer also shows internal rhythms of intensity in calcification. Pore spaces are colonized by abundant small diatoms (higher parts), cyanobacterial filaments (*Ph. incrustatum*, often empty sheaths), and non-phototrophic bacteria (increasingly abundant towards the base) (Pl. 5/1-2). In addition, the lowermost parts are occasionally disrupted by semitubular moulds of insect larvae, which have been observed in several sections. In samples of June the erect *Phormidium* filaments of the biofilm top are already arranged more and more parallel ("*Ph. incrustatum* β") forming a dense meadow, but still with only scattered anhedral microspar.

Samples taken in summer (22.07.1996) show a similar situation as in June. A meadow of parallel erect *Ph. incrustatum* and *Ph. foveolarum* filaments forms the top layer. Only locally radiating filament bushes of *Ph. incrustatum* are still abundant (Pl. 4/6). However, calcite precipitates now form micritic encrustations around *Ph. incrustatum* filaments (Pl. 4/7). The fabric may still be porous as dependent on the density of the filament arrangement. Well illuminated places dominated by *Ph. foveolarum* filaments are encrusted by dense micrite with a vertical fibrous appearance reflecting the erect, densely arranged filaments.

Samples taken in autumn (22.11.1996) show the same micritic, dense to porous top layer of *Ph. incrustatum* and *Ph. foveolarum*, which are still living (Pl. 5/1, 4, 5). However, the upper tips remain uncalcified and a first thin cover of organic detritus, tiny quartz and calcite grains is developed (Pl. 5/3-4). Also, patchy colonies of diatoms

Plate 5 Biofilms and $CaCO_3$ precipitates of the lower creek site, Deinschwanger Bach, Bavaria.

Fig. 1. Vertical section of the upper half of a tufa crust grown of a plastic substrate within 10 months. The sparry spring layer is colonized by *Phormidium incrustatum* (Ph. incr.) filaments and numerous small diatoms (dia). Numerous non-phototrophic bacteria are present, too (not visible on this micrograph). The summer-autumn layer is formed by a dense layer of vertically arranged *Phormidium foveolarum* filaments (Ph. fov.). Note endolithic *Hyella fontana* (hy) within the tufa crust. Autumn (30.09.1997), lower creek section (site 4). Deinschwanger Bach. Epifluorescence micrograph (ex 450-490 nm, em 520-575 nm). Sample RT 97/I-P.

Fig. 2. Same view as in Pl. 5/1 under crossed Nicols to show the location of carbonate precipitates. For scale see Pl. 5/1.

Fig. 3. Overview of a tufa crust grown on a wood substrate (wood) between November 1996 and September 1997. A porous, microsparitic to sparitic spring layer (micrspar) is overlain by a micritic summer-autumn layer (micr). Note internal lamination and erect filamentous structure of the dark summer-autumn layer. The uppermost surface is poorly calcified and rich in detritus. Autumn (30.09.1997), lower creek section (site 4), Deinschwanger Bach. Transmitted light. Sample RT 97/I-H.

Fig. 4. Top of the tufa crust shown in Pl. 5/3. Microcrystalline carbonate precipitated between the densely arranged *Phormidium foveolarum* filaments. Autumn (30.09.1997), lower creek section (site 4), Deinschwanger Bach. Overlay of crossed Nicols and epifluorescence micrograph (ex 450-490 nm, em 520-575 nm). Sample RT 97/I-H.

Fig. 5. Detail showing erect *Phormidium foveolarum* filaments at the top of a 10-month-old tufa crust. Several prostrate *Phormidium incrustatum* filaments (arrows) are visible upon the *Phormidium foveolarum* layer, too. Autumn (30.09.1997), lower creek section (site 4), Deinschwanger Bach. Deconvolved epifluorescence micrograph (ex 450-490 nm, em 520-575 nm). Sample RT 97/I-P.

Fig. 6. Pennate diatoms forming the surface biofilm in winter. The diatoms grow on and between micritic *Phormidium* tubes of late summer-autumn. Winter (01.03.1997), lower creek section (site 4), Deinschwanger Bach. Nomarski optics. Sample RT97/I-W (C 1A)

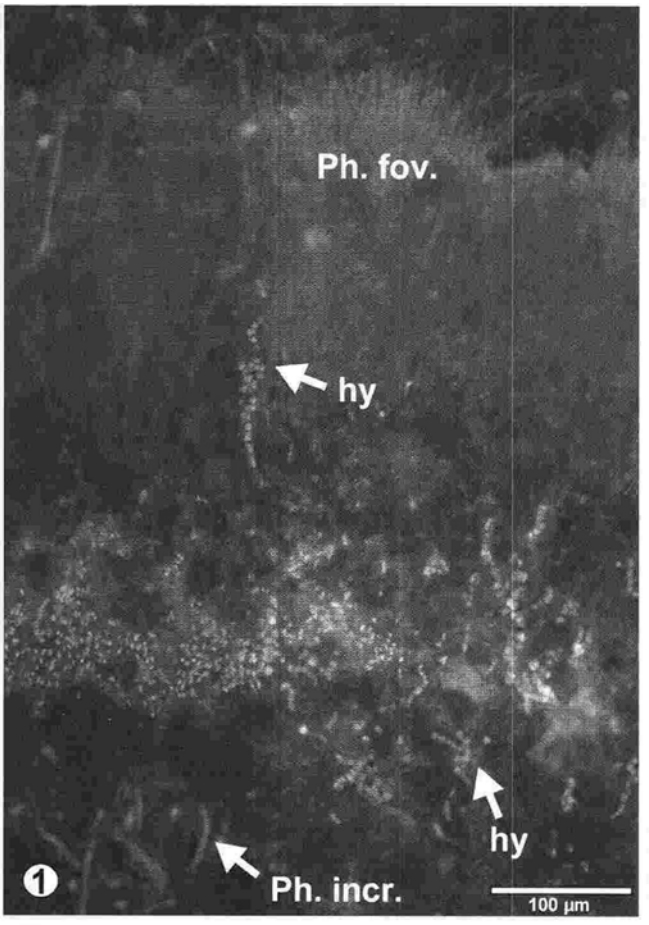
Ph. fov.
hy
hy
Ph. incr.
1
100 µm

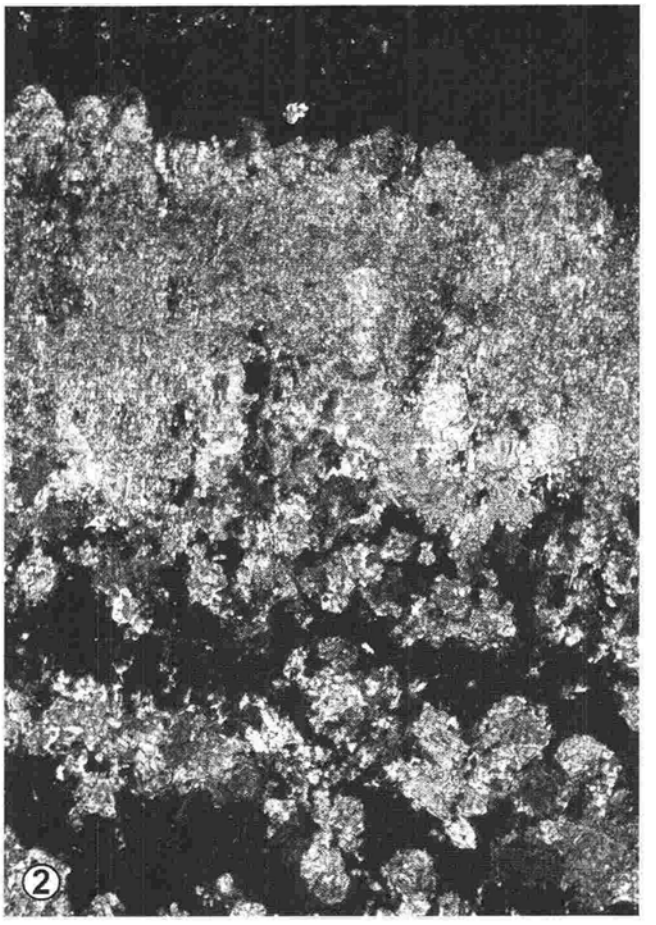
2

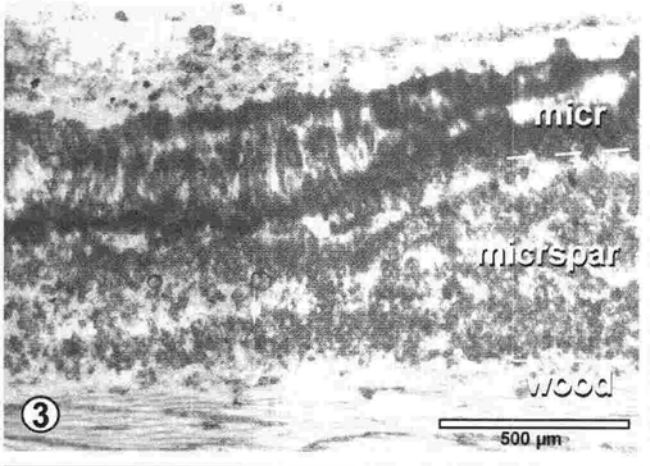
micr
micrspar
wood
3
500 µm

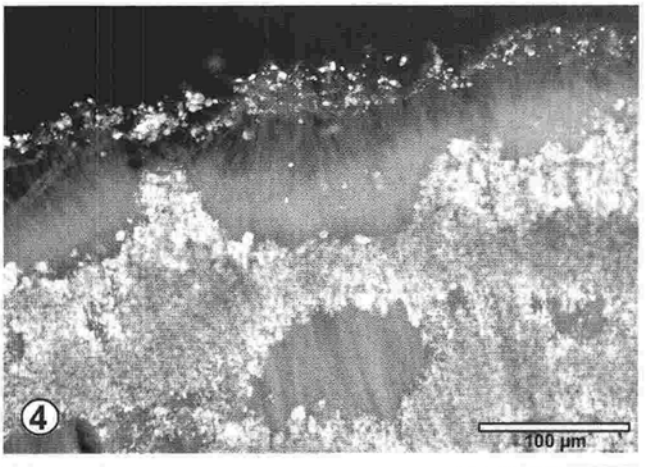
4
100 µm

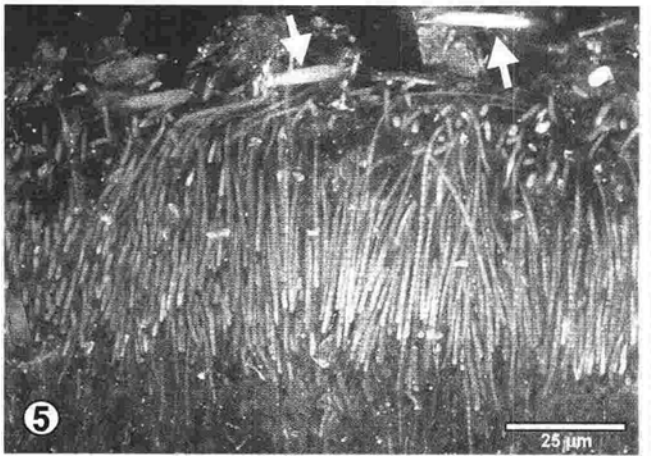
5
25 µm

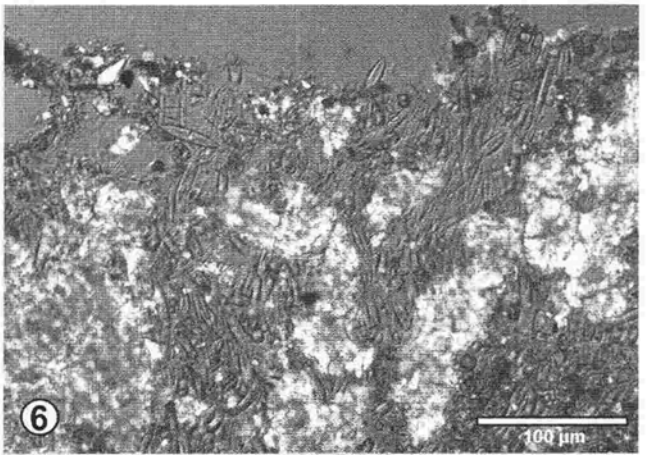
6
100 µm

occur even at well-illuminated places, indicating the transition to the diatom-dominated winter biofilm community. Wherever diatoms occur at the biofilm top or within the crusts, the places remain uncalcified (Pl. 5/1-2).

Samples taken in winter (01./02.03.1997) show a 30-500 µm thick surface layer dominated by pennate diatoms and organic detritus (Pl. 5/6). Some living *Ph. incrustatum* filaments occur in tufa parts of the previous season and are only locally found in the diatom-rich biofilm top. Calcification in the surface layer is restricted to few patches of scattered microspar.

Non-phototrophic bacteria have been found throughout the crusts (Pl. 6/2-3) of all sampling periods. Rod-shaped bacteria of 1x3 µm in size frequently occur at or near the biofilm top. Preliminary results of in-situ hybridizations at hardpart sections revealed that they phylogenetically belong to the β-subclass of the Proteobacteria. At places of abundant bacterial rods, calcification is apparently inhibited (Pl. 6/2-3). Numerous small coccoid bacteria 1 µm in size form microcolonies between cyanobacterial filaments and in pore spaces of deeper crust parts. As in the stromatolitic crusts below the tufa cascade, decaying trichomes of *Ph. incrustatum* are frequently internally colonized by filament-forming bacterial rods and thin filaments of less than 0.5 µm diameter (Pl. 2/9). All these places are essentially free of $CaCO_3$ and crystal aggregates attached to microcolonies have not been found.

7 DIAGENETIC MODIFICATIONS

Diagenetic changes of carbonates precipitated within tufa biofilms potentially start immediately after their formation. Two effects are recognized (Freytet & Verrecchia, 1998, 1999): (1) Equant spar can result from recrystallization of micrite, microsparite, or primary sparite. (2) Micritic to microsparitic fan-like precipitates at cyanobacteria are subject to aggrading neomorphism to result in radial palisadic crystals (often with microlamination) with sweeping extinction when seen under crossed Nicols. The latter effect has been suggested for calcified tufts of *Schizothrix* (Freytet & Verrecchia, 1999), but probably also occurs in calcified bushes of *Phormidium incrustatum* filaments (Janssen et al., 1999).

In the Deinschwanger Bach such diagenetic effects are obvious in sections of subfossil tufa crusts, while they are more difficult to recognize in the recently precipitated carbonate crusts. In 1/2 to 2 years old parts of tufa crusts at the middle and lower creek section, elongated calcite spar crystals form within trichome moulds of *Phormidium foveolarum* and *Phormidium incrustatum*, when the cells are completely decayed, but the sheath and surrounding exopolymers are still present (Pl. 6/4). A similar observation has already been made by Geurts (1976: 13). Furthermore, spring layers of previous year(s) show slightly coarser microspar to spar crystals if compared to surface precipitates

Plate 6 Biofilms, $CaCO_3$ precipitates and diagenetic features at the lower creek site, Deinschwanger Bach, Bavaria.

Fig. 1. Overview of the seasonal lamination in a tufa biofilm crust of the lower creek section (site 4). A microsparitic, porous spring layer grades into a micritic, more dense summer-autumn layer. The surface is covered by a thin winter biofilm with abundant diatoms. A few living *Ph. incrustaum* and *Ph. foveolarum* filaments are still present within the micritic layer of summer-autumn. Winter (01.03.1997), Deinschwanger Bach. Transmitted light. Sample RT97/I-W (T/15a).

Fig. 2. Cyanobacterial filaments (*Phormidium incrustatum*) and associated non-phototrophic bacteria of a tufa crust grown within 10 month on an iron plate. Numerous small coccoid bacteria (cocc) are distributed between the calcareous tubes of filaments. Note rod-shaped bacteria (rods) near the surface of the crust. Lower creek section (site 4), Deinschwanger Bach. Deconvolved epifluorescence micrograph (ex 450-490 nm, em 520-575 nm). Sample RT 97/I-M.

Fig. 3. Same view as in Pl. 6/2 showing the non-phototrophic bacteria in relation to the calcite encrustations of *Phormidium incrustatum* filaments. The bacteria occur in calcite-free spaces. Overlay of crossed Nicols and deconvolved epifluorescence micrograph (ex 450-490 nm, em 520-575 nm).

Fig. 4. Internal calcification of decayed *Phormidium incrustatum* filaments between microspar crystal aggregates of an approximately 4 months old spring layer. Only empty sheaths of *Phormidium* are left, some of them internally filled by elongated calcite crystals. Deeper part of a tufa biofilm crust on wood substrate placed in the lower creek section from 22.11.1996 (winter) to 30.09.1997 (autumn). Overlay of crossed Nicols and epifluorescence micrograph (ex 450-490 nm, em 520-575 nm). Sample RT97/I-H.

Fig. 5. Development of a spar fan by aggrading neomorphism of microspar encrusted, bush-like array of *Phormidium incrustatum* in an approximately 2 years old spring layer. Traces of internally calcified *Ph. incrustatum* filaments are still visible (arrow). Lower creek section (site 4), Deinschwanger Bach. Nomarski optics. Sample RT99/F.

Fig. 6. Subfossil tufa crust at an advanced stage of diagenesis showing an alternation of palisadic spar crystals and micritic zones. Spring (12.06.1999), middle creek section. Transmitted light. Sample RT99/B.

Fig. 7. Detail of radial palisadic spar crystals of a subfossil spar layer. The neomorphic spar shows numerous inclusions, but filament traces of cyanobacteria are absent. Spring (12.06.1999), middle creek section. Crossed Nicols. Sample RT99/B.

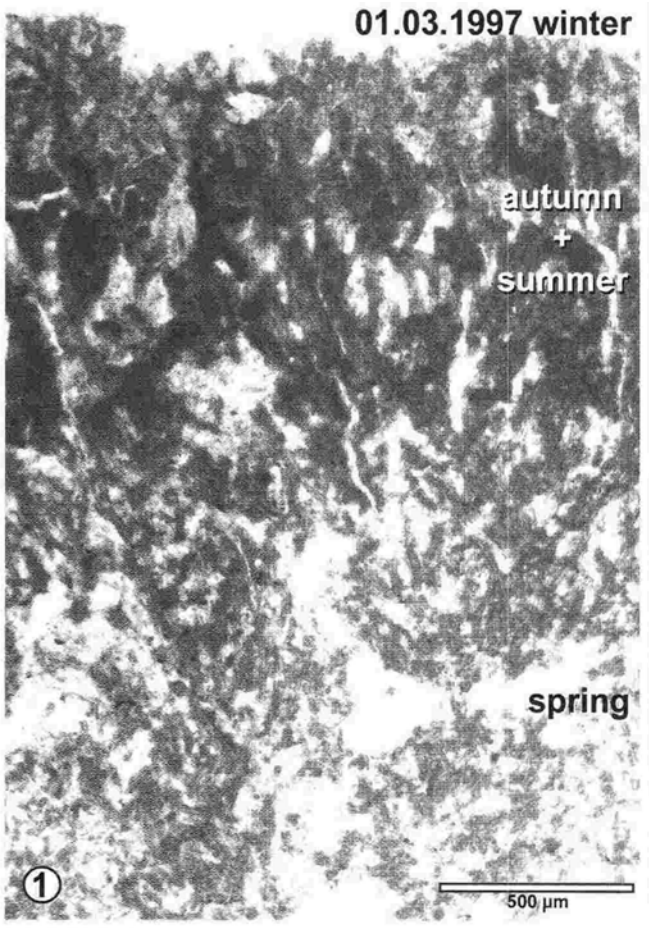
01.03.1997 winter
autumn
+
summer
spring
1
500 µm

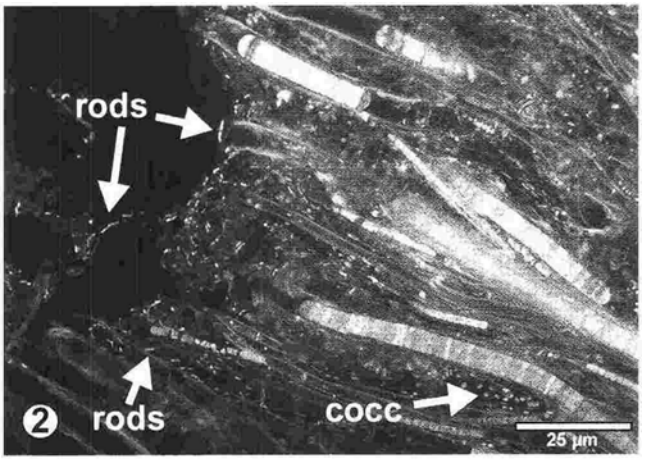
rods
rods
cocc
2
25 µm

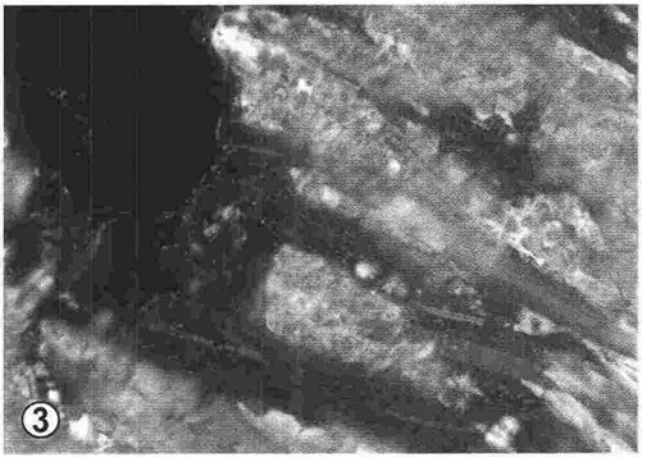
3


4
100 µm

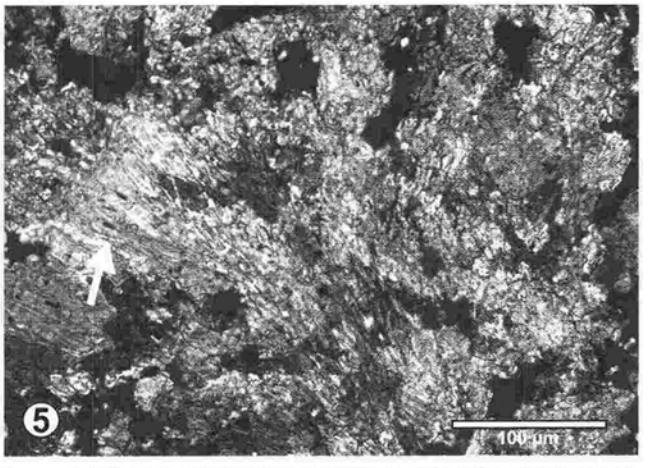
5
100 µm

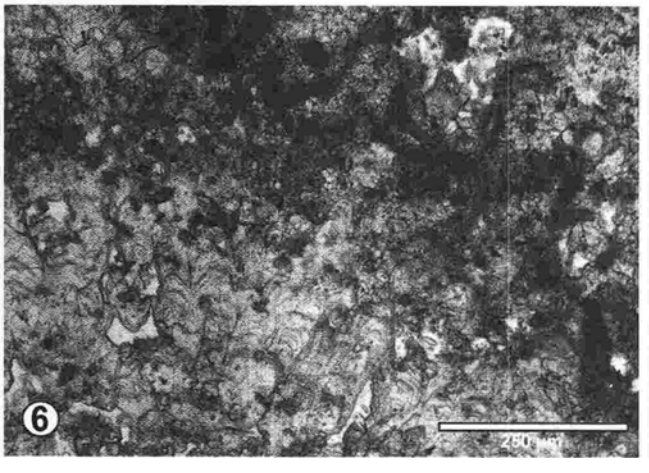
6

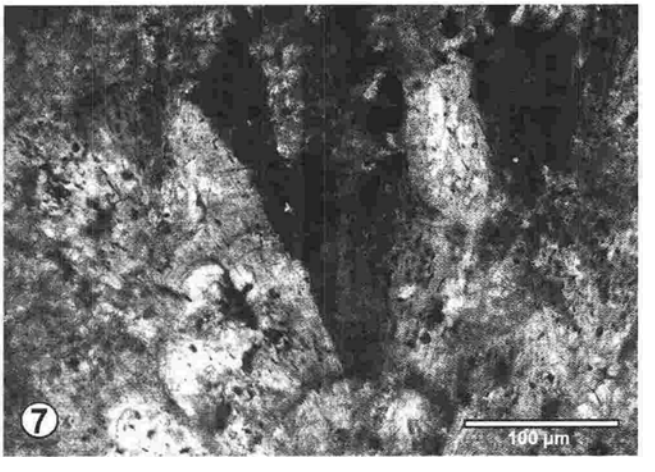
7
100 µm

in present spring layer. More clear is the aggrading neomorphism in bushes of *Ph. incrustatum*. The microspar turns into spar blades when the living trichomes are vanished. During the early stage of this process the calcite moulds of the filaments are still visible (Pl. 6/5), but later also disappear.

Subfossil tufa crusts are commonly composed of continuous spar layers (90 - 350 µm thick) alternating with thinner microcrystalline intercalations (20 - 160 µm thick) (Pl. 6/6). Small inclusions are abundant in the sparite (Pl. 6/7), but filamentous structures that can be attributed to former cyanobacterial filaments are rarely seen. This is consistent with the results of Janssen et al. (1999), who proposed a vanishing of filament traces during the formation of continuous sparry layers. Such layers form by cementation and recrystallization of the initial cyanobacterial micritic bushes upon the disappearance of the organic matter (Janssen et al., 1999).

8 STABLE ISOTOPES OF TUFA CARBONATES AND WATER

Four samples of water and 5 samples of tufa carbonates for $\delta^{13}C$ and $\delta^{18}O$ analysis have been taken at the main spring, the tufa cascade, the middle and lower creek section in June 1999 (Tab. 3). In addition, $\delta^{13}C$ and $\delta^{18}O$ of two samples taken from an artifically placed substrate (collected in 30.09. 1997) have been measured.

The $\delta^{13}C$ data of the dissolved inorganic carbon (DIC) of the waters show a continuous slight increase from -13.28 ‰ at the main spring to less light values of -12.07 ‰ and -11.76 ‰ at the middle and lower creeks section, thereby reflecting the successive degassing of CO_2. On the other hand, the complementary $\delta^{18}O$ data indicate only a mixing of main spring waters and tributaries of side springs. Thus, the physicochemical CO_2-degassing is solely due to the high CO_2 supersaturation, with little or no effect of evaporation.

$\delta^{13}C$ data of calcitic carbonates of the tufa biofilms and moss incrustations of the tufa cascade and the middle creeks section are characterized by uniformly light values of -9.36 ‰ to -10.76 ‰, which are consistent with a pure thermodynamic fractionation, on condition that the $\delta^{13}C$ data of DIC reflect the ratios of waters from which the carbonates were precipitated. Only the biofilm carbonate sample taken at the well illuminated lower creek section shows significantly heavier $\delta^{13}C$ than the corresponding solution, although the $\delta^{18}O$ data exclude evaporation. Spiro & Pentecost (1991) found that the $\delta^{13}C$ of cyanobacterial calcite of a hardwater creek in Yorkshire is on the average 3 ‰ heavier than the stream-average noontime $\delta^{13}C$ of total DIC. Also the cyanobacterial calcite was more than 2 ‰ heavier than biologically unaffected "travertine" on bryophytes (Spiro & Pentecost, 1991). They considered these differences in $\delta^{13}C$ as an effect of photosynthesis. Consequently, the fractionation observed here may point to photosynthetic effect promoting carbonate precipitation of the cyanobacterial biofilms, notwithstanding these spot samples only provide a first indication. However, biofilm carbonates taken from substrate plates (30.09.1997) artificially placed in the lower creek point to the same direction: The cyanobacterial carbonate crust of the well illumated upper side is considerable enriched in ^{13}C compared to the shaded lower side of the plate, while the $\delta^{18}O$ data only slightly differ. This view is consistent with the results of Andrews et al. (1997), who found on basis of $\delta^{13}C$ meausrements of mussel shell aragonite and associated microbial carbonates that a microenvironmental photosynthetic effect is only evident at sites where water flushing rates are low.

9 DISCUSSION: FACTORS AFFECTING THE CARBONATE EQUILIBRIUM

Potential factors affecting the carbonate equilibrium in tufa systems are physicochemical CO_2 degassing, CO_2 fixation by autotrophic organisms (phototrophic cyanobacteria, algae, and bryophytes, chemolithotrophic bacteria), and CO_2 production by chemoorganotrophic bacteria and dark metabolism of phototrophs. Further, the availability and properties of potential nucleation site-forming surfaces has to be taken into account.

In accordance with previous studies on calcareous tufa systems, the rapid decline of pCO_2 along the creek suggests a physicochemically-driven precipitation of $CaCO_3$. The drop from 12900 µatm pCO_2 at the spring to 700 µatm pCO_2 at the middle creek section (Tab. 2) should clearly override any effect of metabolic CO_2 fixation. No precipitation occurs at the main spring, in accordance with the calculated undersaturation. Following CO_2 degassing, clear, well developed spar rhombs form at the tufa cascade upon organic but exopolymer-poor surfaces of mosses (Pl. 2/2-3). The large, idiomorphic crystal habitus suggests a direct, continuous precipitation from the liquid phase starting at few nucleation sites. Tufa crusts 5 m below the cascade already show calcareous tubes which formed upon *Phormidium incrustatum* filaments. Tufa encrustations on moss cauloids of the middle creek section superficially resemble that of the tufa cascade but are composed of hypidiomorphic microspar and spar crystals with abundant microorganisms present (Pl. 3/2-4). Acidic groups abundant in biofilm exopolymers rather than free surfaces of bryophytes are considered as nucleation sites at the middle creek section.

Although the middle and lower creek sites exhibit almost identical water chemistry parameters, differences in calcification intensity have been observed. Carbonate tubes around *Phormidium incrustatum* filaments occur on undersides of artificial substrates, and - less abundant - within natural tufa crusts. Thicker crusts at the lower creek site may be explained by more extensive biofilm development at this well-illuminated place. A larger amount of exopolymers, which are considered to concentrate Ca^{2+} spatially by complexation, might explain a larger amount of $CaCO_3$ precipitated. However, an external encrustation of *Ph. incrustatum* sheaths to result in calcareous tube formation has been observed in crusts of the middle creek section and below the cascade,

sampling site	Sample	description	season, date	$\delta^{13}C$ (DIC;$CaCO_3$) PDB	$\delta^{18}O$ (H_2O) SMOW	$\delta^{18}O$ ($CaCO_3$) PDB	$\delta^{18}O$ ($CaCO_3$) SMOW
main spring	RT99/1	water immediately at spring orifice	spring 12.06.1999	-13,280	-9,940		
tufa cascade	RT99/2	water immediately prior to cascade	spring 12.06.1999	-12,830	-9,530		
middle creek section	RT99/3	water immediately prior to small barrage	spring 12.06.1999	-12,070	-9,790		
lower creek section	RT99/4	water from the middle of the creek	spring 12.06.1999	-11,760	-9,670		
main spring	-	(no $CaCO_3$ precipitates)		-		-	-
tufa cascade	RT99/2a	higher part of tufa cascade, calcite crusted moss	spring 12.06.1999	-9,360		-7,140	23,550
	RT99/2b	lower part of tufa cascade, calcified cyanobacteria crust	spring 12.06.1999	-10,670		-7,270	23,410
middle creek section	RT99/3a	calcite crusted moss of small barrage	spring 12.06.1999	-10,760		-8,130	22,530
	RT99/3b	calcified cyanobacterial biofilm, immediately prior to small barrage	spring 12.06.1999	-10,280		-8,140	22,520
lower creek section	RT99/4	tufa crust on a limestone cobble, calcified cyanobacterial biofilm	spring 12.06.1999	-7,590		-8,040	22,620
lower creek section	RT97/IK oben	calcified cyanobacterial hemisphere (illuminated upper side of artificial substrate)	autumn 30.09.1997	-6,990		-7,480	23,200
	RT97/IK unten	calcified cyanobacterial shrubs (*Phormidium incrustatum*) (shaded lower side of artificial substrate)	autumn 30.09.1997	-10,690		-8,280	22,370

Tab. 3. Stable isotope data of water and biofilm carbonate samples of the Deinschwanger Bach.

too. Initial nucleation at sheath surfaces might possibly be promoted by a photosynthesis-induced pH microgradient. However, the diurnal pH of the macroenvironment is stable (Wedemeyer, 1999) and rapid precipitation precludes a micrite impregnation of the sheaths, so that an external cementation results only. Merz-Preiß & Riding (1999) suggest that sheath impregnation might be restricted to alkaline settings depleted in CO_2, thus, occurs when cyanobacteria switch to bicarbonate fixation and direct release of OH^-. However, in the study they refer to (Merz, 1992), both experiments, inhibition of Photosytem II by DCMU (Dichlorphenyldimethylurea) and inhibition of carboanhydrase by EZ (Ethoxyzolamide), lead to a decrease in the amount of $CaCO_3$ precipitated with increasing concentration of the inhibitors (Merz, 1992: Figs. 5 and 6). The crucial point is, whether EZ really inhibits a separate HCO_3^- transport system or a combined CO_2/HCO_3^- pump in the cyanobacteria in question. Thus, further experimental studies are necessary to prove their suggestion.

The role of bacteria as active agents in the formation of tufa carbonates is difficult to assess. In the Deinschwanger Bach, most of the non-phototrophic bacteria apparently thrive on exopolymers and decay products of the cyanobacteria, hence, are likely chemoorganotrophs. They therefore potentially rather produce than consume CO_2, and may lower $CaCO_3$ supersaturation. Szulc & Smyk (1994) isolated several bacteria from cyanobacterial biofilms of a slope spring tufa in Poland. Although 7 of the 8 species mentioned are chemoorganotrophic and largely considered to dissolve $CaCO_3$, the presence of numerous bacteria-shaped rods ("baculiform") has been taken as indicative for a bacterially controlled calcification. "Baculiform" calcite rods are interpreted to result from autolytically induced cell calcification. Szulc & Smyk (1994) postulated a decisive role of bacteria in the calcification of tufa microbial mats in their investigated case study. With regard to a bacterial CO_2 assimilation that may effectively cause precipitation, this suggestion is speculative and remains to be shown. In any case, in-situ hybridizations are necessary to localize and prove the presence of active bacterial cells of the different species within the crusts. The application of pH-sensitive microelectrodes or fluorochromes may be used to test the supposed microscale interactions (see e.g., Merz et al., 1995). Experimental studies by Caudwell (1987) indeed indicate a complex relationship of bacterial carbohydrate consumption, pH decrease, and subsequent alkalinization that may occur within tufa biofilm microenvironments. However, even in the case study of Caudwell (1987) pre-existing carbonate in cyanobacterial sheaths is only dissolved and reprecipitated by the non-phototrophic bacteria.

10 DISCUSSION: SEASONAL LAMINATION

In general, seasonal lamination in *Phormidium* tufa crusts reflects the alternation of (1) light, porous layer made of scattered calcified bundles (*Ph. incrustatum* α) separated by wide cavities and detrital components, and (2) dark, coherent layers with densely arranged, erect filaments (*Ph.*

incrustatum β) (Geurts, 1976; Monty, 1976; Freytet & Plet, 1996; Janssen et al., 1999). Light, porous laminae show pollen spectra dominated by plants flowering in summer and autumn, while dark, dense laminae are characterized by pollen of plants flowering in spring (Geurts, 1976: 18). By refering to Geurts (1976), Monty (1976) regarded porous laminae having formed during May to January, whereas he assigned dense laminae to the period February to April. Lamination in the investigated tufa crusts has been observed mainly in lower creek section samples, but even there, it is not always well developed due to lateral changes in biofilm composition. Sampling during all four seasons and artificially placed substrate plates give evidence for an alternation of different layers which differs from previous interpretations of seasonal laminae formation (Pl. 6/1).

In the Deinschwanger Bach, spring biofilms are characterized by erect bushes of *Ph. incrustatum* filaments, and diatoms occupying pore spaces in deeper biofilm parts. On the other hand, tufa biofilms from localities in Belgium also show bushes of erect *Ph. incrustatum* filaments, but are apparently heavily micrite-encrusted to result in a dense spring lamina (Janssen et al., 1999). However, calcification in the Deinschwanger Bach is less intense and characterized by loosely distributed microspar (Pl. 4/5), leading to the formation of a rather porous spring layer (Pl. 5/3, 6/1). One may speculate, if optimum conditions during spring may promote the production of highly hydrated, less acidic exopolymers, which provide fewer nucleation sites.

Summer-autumn samples from the Deinschwanger Bach show a micritic and commonly dense top layer, which encrusts densely arranged filaments of *Ph. foveolarum* and *Ph. incrustatum* β (Pl. 4/6-7, 5/1-5). The change from microspar to micrite may reflect a chemical change in the produced exopolymers: restricted availability of nutrients (increase of metabolic stress) may lead to exopolymers with higher concentrations in carboxylate. This suggestion is speculative for cyanobacteria, but has been shown for bacteria (Uhlinger & White, 1983). Increased illumination during summer may further amplify this effect. In Belgian tufa biofilms, the porous laminae (with *Ph. incrustatum* α, detrital components) are considered to form in summer (Janssen et al., 1999), as based on palynological investigations (Geurts, 1976). This contradiction may be explained by the possibility that seasonal changes in biofilm composition and physicochemical parameters may not be the same in different creeks in question. As an alternative explanation, pollen of summer and autumn may stick only superficially to autumn biofilms, but are overgrown to be incorporated in the organic mucus in winter.

Winter biofilms in the Deinschwanger Bach are dominated by diatoms covering a still living, already micrite-encrusted *Ph. incrustatum - Ph. foveolarum* layer (Pl. 5/6, 6/1). The diatom layer appears to be free of current precipitates. However, it remains unclear, if calcification still slightly proceeds in the *Ph. incrustatum - Ph. foveolarum* layer below the diatoms. In general, calcification during winter does not appear to cease completely (Janssen et al., 1999).

A seasonal lamination has also been described from *Schizothrix*-tufa crusts from the Pieniny Mountains in southern Poland (Szulc & Smyk, 1994). Again in contrast to the present study, dense laminae are assigned to spring and porous laminae to summer, as based on SEM investigations of samples taken in January, April, July, and September. During spring intensive growth of diatoms and cyanobacteria should result in intensive calcification and hence, compact and coalescent laminae. During summer the decline in diatoms and a rise in temperature should explain that calcified envelopes become more loose and a porous lamina forms. In autumn and winter carbonate production should dimish gradually. In addition, a weak dissolution due to chemoorganotrophic bacteria and/or slight acidic coating of diatoms is described, although calcification should proceed (Szulc & Smyk, 1994). However, for a comparison with the present results from the Deinschwanger Bach thin sectioning of fixed, resin-embedded material from the Pieniny Mountains is necessary.

11 CONCLUSIONS

(1) Present-day $CaCO_3$ precipitation within the Deinschwanger Bach is evident by tufa crusts on artificial substrates placed in the creek for 10 months. Carbonate tufa crusts up to 1.5 mm thickness formed between November 1996 and September 1997.

(2) Hydrochemical data and calculations indicate that tufa deposition in the Deinschwanger Bach is physicochemically driven by CO_2 degassing. There is no evidence for a significant influence of photosynthetic CO_2 fixation on the macroscale carbonate equilibrium.

(3) Stable carbon isotope data indicate a minor photosynthetic fractionation with regard to the precipitated carbonates, but only for the lower creek section. Nonetheless, the effect is not strong enough to cause a sheath impregnation by $CaCO_3$ at the cyanobacteria.

(4) Lower creek tufa crusts of *Phormidium incrustatum - Ph. foveolarum* - diatom biofilms show a seasonal lamination. Highly porous spring laminae are composed of loosely distributed microspar and hypidiomorphic microspar, whereas summer-autumn laminae are microcrystalline and commonly dense. This change in fabric reflects an alternation of spring biofilms with *Ph. incrustatum* α, summer-autumn biofilms with *Ph. incrustatum* β and *Ph. foveolarum*, and winter biofilms rich in diatoms and organic detritus.

(5) The endolithic cyanobacterium 3 and *Hyella fontana* occur within limestone substrates but also within constructive tufa crusts, thereby contributing to the maintenance of porosity.

(6) Non-phototrophic bacteria occur in large numbers in *Ph. incrustatum - Ph.* foveolarum - diatom biofilms. Most of the bacteria digest exopolymers and dead cyanobacterial cells. This EPS degradation rather results in secondary Ca^{2+} release and microscale decrease in $CaCO_3$ supersaturation by CO_2 production. Thus, these bacteria are unlikely to cause $CaCO_3$ precipitation by a microscale

rise in supersaturation, but possibly contribute to the maintenance of porosity as long as they metabolize.

(7) The presence and abundance of chemolithotrophic bacteria within natural biofilm samples remains to be shown.

(8) First diagenetic features are calcite precipitates within empty sheaths of decayed trichomes and occur already after 4 months. Successive aggrading neomorphism in microspar layers leads to subfossil tufa crusts composed of palisadic sparite layers and thin micritic intercalations.

ACKNOWLEDGEMENTS

The study was supported by the Deutsche Forschungsgemeinschaft (SFB 468-A1, Re 665/12-1 LEIBNIZ-Award). Microbiological parts significantly benefited from discussions with Dipl.-Biol. Gabriela Schumann-Kindel and Dr. Werner Manz (Microbiology, TU Berlin). GA thanks Dieter Kötting (Max-Planck-Institut für Biophysikalische Chemie, Göttingen) for teaching in ultrathin sectioning, access and introduction to the TEM. Dr. Christian Böker, Carl Zeiss GmbH Göttingen, provided CLSM images of endolithic cyanobacteria. Dr. Andreas Reimer (IMGP, Göttingen) is gratefully acknowledged for support in hydrochemistry analysis and introduction to the program PHREEQE. We are grateful to the reviewers Dr. P. Freytet (Verrières-le-Buisson) and Dr. Martina Merz-Preiß (Marburg) for their helpful suggestions and corrections.

REFERENCES

Anagnostidis, K. & Komárek, J. (1988): Modern approach to the classification system of cyanophytes: 3 - Oscillatoriales. - Archiv für Hydrobiologie, Suppl. **80** (Algological Studies 50-53), 327-472, Stuttgart.

Andrews, J.E., Riding, R. & Dennis, P.F. (1997): The stable isotope record of environmental and climatic signals in modern terrestrial microbial carbonates from Europe. - Palaeogeogr. Palaeoclimatol. Palaeoecol., **129**, 171-189, Amsterdam.

Arp, G., Hofmann, J., & Reitner, J. (1998): Microbial fabric formation in spring mounds ("microbialites") of alkaline salt lakes in the Badain Jaran Sand Sea, PR China. - Palaios **13**, 581-592, Tulsa.

Arp, G., Thiel, V., Reimer, A., Michaelis, W., & Reitner, J. (1999): Biofilm exopolymers control microbialite formation at thermal springs discharging into the alkaline Pyramid Lake, Nevada, USA. - Sed. Geol. **126**, 159-176, Amsterdam.

Bögli, A. (1978): Karsthydrographie und physische Speläologie. - 292 p., Berlin (Springer).

Caudwell, C. (1987): Étude expérimentale de la formation de micrite et de sparite dans les stromalites d'eau douce à *Rivularia*. - Bull. Soc. géol. France, **8**, t.III, no 2, 299-309, Paris.

Freytet, P. & Plet, A. (1996): Modern freshwater microbial carbonates: the *Phormidium* stromatolites (tufa-travertine) of southeastern Burgundy (Paris basin, France). - Facies **34**, 219-238, Erlangen.

Freytet, P. & Verrecchia, E.P. (1998): Freshwater organisms that build stromatolites: a synopsis of biocrystallization by prokaryotic and eukaryotic algae. - Sedimentology **45**, 535-563, Oxford.

Freytet, P. & Verrecchia, E.P. (1999): Calcitic radial palisadic fabric in freshwater stromatolites: diagenetic and recrystallized feature or physicochemical sinter crust? - Sed. Geol. **126**: 97–102

Fritsch, F.E. (1949): The lime-encrusted *Phormidium*-community of British streams. - Verhandlungen Internationale Vereinigung für Theoretische und Angewandte Limnologie, **10**, 141-144, Stuttgart.

Fritsch, F.E. (1950): *Phormidium incrustatum* (Nalg.) Gom., an important member of the lime-encrusted communities of flowing waters. - Biologisch Jaarboek, **17**, 27-39, Den Haag.

Geitler, L. (1932): Cyanophyceae. - Rabenhorst's Kryptogamen-Flora von Deutschland, Österreich und der Schweiz, 2nd ed., **14**, 1196 p., Koenigstein (Reprint 1985, Koeltz Scientific Books).

Golubic, S. (1973): The relationship between blue-green algae and carbonate deposits. - In: Carr, N.G. & Whitton, B.A. (eds.): The biology of blue-green algae. - Bot. Monogr. **9**, 434-472, Oxford (Blackwell).

Grüninger, W. (1965): Rezente Kalktuffbildung im Bereich der Uracher Wasserfälle. - Abhandlungen zur Karst- und Höhlenkunde, Reihe E (Botanik) **2**, 1-113, München.

Herman, J.S. & Lorah, M.M. (1987): CO_2 outgassing and calcite precipitation in Falling Spring Creek, USA. - Chem. Geol. **62**, 251-262, Amsterdam.

Herman, J.S. & Lorah, M.M. (1988): Calcite precipitation rates in the field: measurement and prediction for a travertine-depositing stream. - Geochim. Cosmochim. Acta **52**, 2347-2355, Oxford.

Irion, G. & Müller, G. (1968): Mineralogy, petrology and chemical composition of some calcareous tufa from the Schwäbische Alb, Germany. - In: Müller, G. & Friedman, G.M. (eds.): Recent developments in carbonate sedimentology in central Europe, 157-171, Heidelberg (Springer).

Janssen, A., Swennen, R., Podoor, N. & Keppens, E. (1999): Biological and diagenetic influence in Recent and fossil tufa deposits from Belgium. - Sed. Geol., **126**, 75–95, Amsterdam.

Jensen, T.E. (1985): Cell inclusions in the cyanobacteria. - Archiv für Hydrobiologie, Suppl. **71** (Algological Studies 38-39), 33-73, Stuttgart.

Kann, E. (1973): Bemerkungen zur Systematik und Ökologie einiger mit Kalk inkrustierter *Phormidium*arten. - Schweiz. Z. Hydrol., **35**, 141-151, Basel.

Manz, W., Arp, G., Schumann-Kindel, G., Szewzyk, U. & Reitner, J. (2000): Widefield deconvolution epifluorescence microscopy combined with fluorescent in situ hybridization shows the spatial arrangement of bacteria in sponge tissue. - Journal of Microbiological Methods **40**, 125-134, Amsterdam.

Merz, M.U.E. (1992): The biology of carbonate precipitation by cyanobacteria. - Facies **26**, 81-102, Erlangen.

Merz, M.U.E., Schlue, W.R. & Zankl, H. (1995): pH-measurements in the sheath of calcifying filamentous cyanobacteria. - Bull. Inst. océanogr. Monaco no. spec. **13**, 61-117, Monaco.

Merz-Preiß, M.U.E. & Riding, R. (1999): Cyanobacterial tufa calcification in two freshwater streams: ambient environment, chemical thresholds and biological processes. - Sed. Geol. **126**, 103-124, Amsterdam.

Monty, C.L.V. (1976): The origin and development of crytalgal fabries. - In: Walter, M.R. (ed.): Stromatolites. - Dev. Sedimentol. **20**, 193-249, Amsterdam (Elsevier).

Parkhurst, D.L., Thorstenson, D.C. & Plummer L.N. (1990): PHREEQE - A computer program for geochemical calculations. (Conversion and upgrade of the prime version of PHREEQE to IBM PC-compatible systems by Tirisanni J.V. & Glynn P.D.). - U.S. Geol. Surv. Water-Res. Invest. Rep. **80-96**, 197 p., Denver.

Pentecost, A. (1978): Blue-green algae and freshwater carbonate deposits. - Proc. Roy. Soc. London B **200**, 43-61, London.

Pentecost, A. (1985): Association of cyanobacteria with tufa deposits: identity, enumeration, and nature of the sheath material revealed by histochemistry. - Geomicrobiol. J. **4**, 285-298, New York.

Pentecost, A. & Riding, R. (1986): Calcification in cyanobacteria.

- In: Leadbeater, B.S.C. & Riding, R. (eds.): Biomineralization of lower plants and animals, 73-90, Oxford (Clarendon).

Pentecost, A. & Therry, C. (1988): Inability to demonstrate calcite precipitation by bacterial isolates from travertine. - Geomicrobiol. J. **6**, 185-194, New York.

Persoh, D. (1998): Onkoide in Moosach und Sempt. Entstehung, Struktur und Verbreitung. - 63 p., unpublished diploma thesis TU München.

Pia, J. (1926): Pflanzen als Gesteinsbildner. - 355 p., Berlin (Borntraeger).

Pia, J. (1933): Die rezenten Kalksteine. - Zeitschrift fuer Kristallographie, Mineralogie und Petrographie, Abt. B, Ergänz. Bd. 1: 420 p., Leipzig.

Rott, E. (1994): Der Algenaufwuchs in der Oberen Alz (Oberbayern). - Ber. nat.-med. Verein Innsbruck **81**, 229-253, Innsbruck.

Scharfenberg, N. (1994): Die Algenflora eines Kalkflachmoores in der thüringischen Rhön und einer Kalktuffbildung im Spessart. - 98 p., 9 pls., unpublished diploma thesis Julius-Maximilians-Universität Würzburg.

Schmidt-Kaler, H. (1974): Geologische Karte von Bayern 1 : 25 000 Erläuterungen zum Blatt Nr. 6634 Altdorf. - 152 p., 1 map, 6 inserts, München (Bayerisches Geologisches Landesamt).

Spiro, B. & Pentecost, A. (1991): One day in the life of a stream - a diurnal inorganic carbon mass balance for a travertine-depositing stream (Waterfall Beck, Yorkshire). - Geomicrobiol. J., **9**, 1-11, New York.

Stirn, A. (1964): Kalktuffvorkommen und Kalktufftypen der Schwäbischen Alb. - Abhandlungen zur Karst- und Höhlenkunde, Reihe E (Botanik) **1**, 1-92, München.

Stumm, W. & Morgan, J.J. (1996): Aquatic Chemistry. Chemical equilibria and rates in natural waters. - 3rd ed., 1022 p., New York (Wiley).

Symoens, J.J. (1947): *Lyngbya calcarea* (Tilden) Symoens, nov. comb. (= *Lyngbya Martensiana* Menegh. var. *calcarea* Tilden) en Europe occidentale. - Bulletin de la Société botanique de France, **94**, 210-210, Paris.

Symoens, J.J. (1957): Les eaux douces de l'Ardenne et des régions voisines: les milieux et leur végétation algale. - Bulletin de la Société Royale de Botanique de Belgique, **89**, 111-314, Bruxelles.

Szulc, J. & Smyk, B. (1994): Bacterially controlled calcification of freshwater *Schizothrix*-stromatolites: an example from the Pieniny Mts., Southern Poland. - In: Bertrand-Sarfati, J. & Monty, C. (eds.): Phanerozoic Stromatolites II, 31-51, Dordrecht (Kluwer).

Uhlinger, D.J. & White, D.C. (1983): Relationship between physiological status and formation of extracellular polysaccharide glycocalyx in *Pseudomonas alantica*. - Appl. Envirnm. Microbiol., **45**, 64-70, Washington.

Usdowski, E., Hoefs, J. & Menschel, G. (1979): Relationship between ^{13}C and ^{18}O fractionation and changes in major element composition in a Recent calcite-depositing spring. A model of chemical variations with inorganic $CaCO_3$ precipitation. - Earth Planet. Sci. Lett. **42**, 267-276, Amsterdam.

Wallner, J. (1934a): Über die Beteiligung kalkablagernder Pflanzen bei der Bildung südbayerischer Tuffe. - Bibliotheca Botanica **110**, 1-30, Stuttgart.

Wallner, J. (1934b): Über die Bedeutung der sog. Chironomidentuffe für die Messung der jährlichen Kalkproduktion durch Algen. - Hedwigia **74**, 176-180, Dresden.

Wallner, J. (1935): Über die Beteiligung kalkablagernder Algen am Aufbau der Chironomidentuffe. - Beihefte zum Botanischen Centralblatt **54**, Abt. A, 142-150, Dresden.

Wedemeyer, N. (1999): Biologische und abiologische Faktoren fluviatiler Karbonatkrusten ("Kalktuffe") des Rohrenstädter Tals (Frankenalb, Nordbayern). - 122 p., 23 pls., 2 inserts, unpublished diploma thesis Universität Göttingen.

Winsborough, B.M., Seeler, J.S., Golubic, S., Folk, R.L. & Maguire, B. Jr (1994): Recent fresh-water lacustrine stromatolites, stromatolitic mats and oncoids from Northeastern Mexico. - In: Bertrand-Sarfati, J. & Monty, C. (eds.): Phanerozoic stromatolites II. - 71-100, Dordrecht (Kluwer).

Manuscript received July 23, 2000
Revised manuscript accepted December 2, 2000